SSRG International Journal of Electrical and Electronics Engineering
ISSN: 2348-8379/ https://doi.org/10.14445/23488379/IJEEE-V13I2P103

Volume 13 Issue 2, 38-59, February 2026

Original Article

Investigation of Smart Inverter Integration within a Planned Load Shedding Management Framework: A Case Study of the Tunisian LV Power Distribution System

Asma Ben Chida[1*], Ghada Boukettaya[1], Rafik Cherni[2]

[1]*Electrical Engineering Department, Laboratory of Electrical Systems and Renewable Energies (LSEER), University of Sfax, National Engineering School of Sfax (ENIS), 3038 Sfax, Tunisia.*
[2]*MICROGRIDS Laboratory, Tunisian Company of Electricity and Gas (STEG).*

[*]*Corresponding Author : asma.benchida@enis.tn*

Received: 12 November 2025 Revised: 17 December 2025 Accepted: 14 January 2026 Published: 17 February 2026

Abstract *- Over recent decades, renewable energy sources, particularly solar energy, have become increasingly viable. In response to Tunisia's growing energy deficit, this study explored the integration of Smart Inverters (SIs) within a planned Load-Shedding (LS) framework to manage consumption peaks in Low-Voltage (LV) distribution networks. SI control is based on the synchronverter, a control strategy of a grid-forming inverter that allows the inverter to act as a voltage source and emulate the virtual inertia of a Synchronous Generator (SynGen) through the DC-link capacitor. A control strategy was proposed, combining the synchronverter with an Energy Management System (EMS) that handled the voltage regulation. This innovative approach, leveraging day-ahead data to plan the next day's LS, dynamically manages Volt-Var activation and prioritizes customer connection or disconnection according to a predefined priority framework. This ensures the continuous supply to critical customers during islanding events and enhances the system's resilience under peak consumption conditions. Simulations conducted using MATLAB software proved the effectiveness of the proposed strategy, highlighting its ability to improve voltage stability, optimize load management, and increase the contribution of Photovoltaic (PV) systems in Tunisia's LV networks. The results highlighted the potential of this integrated approach to support sustainable energy management, reduce energy deficit, and enhance the overall reliability of Tunisia's electricity grid under a planned LS.*

Keywords *- PV, SI, EMS, Planned LS, Tunisian LV distribution network.*

1. Introduction

The increased price of fossil fuels and their adverse effects on the environment have increased the move to renewable energy all over the world. One of the most burning issues today is pollution and the energy crisis that has compelled policymakers and researchers to seek sustainable solutions [1-3]. The alternative source, which is clean and reliable, is renewable energy, especially solar PV, because it does not release greenhouse gases and it also has long-term economic benefits [4]. As a result, a number of governments are supporting solar PV by offering incentives and policies that lower the costs of installation and subsidize its use in the national energy mixes [5]. Solar PV installation has expanded at an alarming rate globally, and it has become one of the fastest-growing sources of energy. The International Energy Agency (IEA) forecasts that solar PV will have overtaken coal in installed capability by 2027 to become the biggest energy source on earth [5]. Recent statistics confirm the record values of installed PV capacity in 2022, 240 GWp of the sum total of the installed capacity was added worldwide, which is equivalent to a cumulative capacity of 1,185 GWp [6]. China is the market leader with 106 GWp of the capacity added, and Spain made a 19.1% penetration rate. In general, PV is now contributing 6.2% of electricity in the world [6], which is indicative of the growing relevance of solar energy in national and global energy transitions. Tunisia is a pioneer in the adoption of renewable energy in the Arab region, with its vision dating back to the 1980s. In 1985, with the creation of the National Agency for Energy Management (ANME), the attempts at diversifying the energy mix, as well as making it efficient, started taking an organized form [7]. Tunisia, which has been confronted with an increasing energy shortage since the 2000s, introduced the Tunisian Solar Plan (PST) as one of the major tools to include renewable electricity generation into the energy system [7, 8]. By 2030, the PST targets 3,815 MW of renewable capacity, of which 1,510 MW of PV (almost one-third of the entire power mix) is targeted [7]. The plan identifies grid-connected power generation technologies (PV, wind, Concentrated Solar Power (CSP), and biomass) as its priorities.

In addition to environmental advantages, the PST will enhance energy self-sufficiency, improve the balance of trade, and increase investment in the power industry [8]. To hasten the process, the Tunisian government in 2018 adopted an action plan that presented short and medium-term plans to address regulatory, financial, and infrastructural obstacles [8]. However, there are still difficulties in the scaling up of the projects, funding of the projects, and the modernization of the grid to meet the requirements of intermittent renewable generation. This paper is interested in the position of solar PV in the Tunisian renewable energy plan, focusing on both the opportunities and the challenges. Through the analysis of the development of Tunisia, the paper will offer an understanding of how developing nations can use solar PV in order to minimize reliance on fossil fuels, to increase energy security, and to facilitate sustainable global objectives. This paper aims to discuss the place of solar PV in the renewable energy plan in Tunisia, and the opportunities and obstacles of implementing it. Therefore, the Tunisian PV market is gradually developing not only in LV but also in Medium-Voltage (MV) areas. The LV PV systems reached a capacity of 130,000 kWp in 2021. As for MV, the total PV capacity reached 68 MWp by the end of 2022, supplied by 302 authorized PV projects [9].

Tunisia, among the pioneer Arab countries to consider renewable energies, is unfortunately suffering from significant concern regarding its current energy situation, with an energy deficit contributing to 54% of the total deficit at the end of September 2023 [10]. According to the report on the energy situation up to October 2023, published by the Ministry of Industry, Mines and Energy, Tunisia's energy dependency rate stood at 51% at the end of October 2023 [11]. The number of PV installations has risen at the end of 2023. About 201 MWp of PV roofs were installed in the residential sector, and 311 authorisations were issued, with a cumulative capacity of 89 MWp, across the industrial, tertiary, and agricultural sectors [11].

As of July 2023, Tunisia imposed three electricity consumption peaks as a result of the active use of air conditioning. Due to this dire state of affairs, the Tunisian Company of Electricity and Gas (STEG) has initiated periodical LS in some of the areas to alleviate the system and prevent major power failures [12]. A programme of periodic LS, 15 -30 minutes, was introduced by STEG in the summer of 2024, predicting such extreme scenarios as blackouts in sensitive facilities and important installations of the country [13]. Clearly, there must be solutions to decrease the energy shortage in Tunisia, and one of the approaches can be to increase the proportion of renewable energies in the national primary energy sources. But that is not enough. It is also important to think of minimising the energy consumption using conscientious activities to achieve an effective and dynamic energy management [14]. Furthermore, the idea of electric mobility exploration and development is a crucial direction to consider in the process of achieving sustainable energy solutions [15]. In spite of all the benefits of solar PV energy, there are still some constraints and limitations that exist [16-18]. Even though Under-Frequency LS (UFLS) and Under-Voltage LS (UVLS) methods are used in most exciting strategies, there are serious limitations. They are not flexible, adaptable, and coordinated, and are often applied to hierarchical structures to provide priority loads to high-priority tasks. They mostly rely on time constant adjustments, which restrict their capacity to adjust to sudden shifts in the working conditions [19-22].

Furthermore, it has been found that combining optimization schemes, including Artificial Bee Colony (ABC) algorithm and Fast Voltage Stability Index (FVSI) to prioritise weak buses, has a better performance in preserving critical loads and avoiding voltage collapse than traditional methods, such as Genetic Algorithm (GA), Particle Swarm Optimization (PSO) and a combination of them (GA-PSO) [23, 24]. These methods are complicated to use and are dependent on real-time statistics, which are not always available in Tunisian networks. Also, it was proposed to use hybrid EMSs that combine PV panels, Battery Energy Storage Systems (BESS), and other sources of generation (e.g., diesel generators) to reduce LS [25-27].

Although the recent work has attempted to incorporate SIs as a part of LV systems, the literature usually does not look at the integrated control systems of synchronverter technology and the EMSs during planned LS. This paper closes such a gap by constructing an effective, simulated-tested framework custom-designed to suit the LV grid of Tunisia that shows enhanced stability of the voltages and availability of supply to customers. The remaining part of the paper was structured in the following way. Section 2 presented the SI control, which provided a technical description of the synchronverter and a Volt-Var control. Section 3 has presented the LS application in the Tunisian LV grid, focusing on the presented methodology. Section 4 offered the simulation results and discussions of the results. Section 5 was the last section that was used to conclude the paper.

2. Smart Inverter Control: An Advanced Grid-Connected Inverter

Inverters have found wide application in the electrical systems industry with applications in PV systems, wind generators, gas micro-turbines, and energy storage devices. Inverters are important devices with each one having a special purpose, so they are classified as grid-forming, grid-following, and grid-supporting [28-31]. A grid-forming inverter is an autonomous setup that creates and controls voltage and frequency in a Microgrid (MG), not capable of working in parallel with other grid-forming inverters. A grid-following inverter (or grid-feeding inverter), on the other hand, puts energy generated by renewable sources into the existing power grid so that it can be distributed more widely. It uses a Phase-Locked Loop (PLL) to keep synchronised with the network by tracking the phase angle of the grid voltage. Grid-supporting inverter is designed to work in both connected and disconnected modes, offering more services such as voltage regulation, frequency control, and reactive power compensation.

Power electronics are also being considered as a viable option in bringing renewable energy systems into the power grid on a large scale. Technological changes in the last couple of decades have contributed to the high usage of power electronic devices. That is why scientists and industrialists are interested in the improvements and economic and technical solutions of the management of electrical energy [32]. Being one of the essential elements of the Distributed Generation (DG) connection with the electrical grid, the inverter transforms the direct current into alternating one and controls the maximum power of the DG. But inverters do not have the flexibility to effectively cope with the augmented infiltration of renewable energy and confirm the dependability and stability of the system. The inverters, therefore, need advanced features that will make them better in terms of capabilities and capacities. The traditional inverters must progress to smart devices to address such concerns. Now the trend is shifted to the development of SIs, which are oriented more towards the standardised control and interoperability functions in order to meet the network standards, thereby assuring the network security, stability, and reliability [33, 34].

In this context, grid codes and standards require that the inverter detect abnormal conditions in the grid and respond autonomously by making the appropriate decision. Consequently, the regulation of the DG's interconnection to the grid, including grid support functions and ancillary services, will be guaranteed. According to California’s Rule 21 [35], the interconnection tariff levied by the California Public Utility Commission (CPUC), the basic definition of an SI is “a generating facility’s inverter that performs functions that, when activated, can autonomously contribute to grid support during excursions from normal operating voltage and frequency system conditions by providing: dynamic reactive/real power support, voltage and frequency ride-through, ramp rate controls, communication systems with the ability to accept external commands and other functions”. To streamline the SI process, the IEEE has introduced a set of standards known as IEEE Std 1547. The interconnection and interoperability standards described in IEEE Std 1547-2018 for Distributed Energy Resources (DERs) within electric power systems have undergone recent revisions and publications to incorporate advanced features requested by utilities. It enables DERs to address network needs by riding through abnormal voltage/frequency conditions, regulating voltage through reactive power adjustment, and meeting interoperability/communication requirements [36].

Several studies have investigated the topical issue of SI. Mamadaminov also published new distributed solar generation inverters with advanced features and new control measures, including reactive power control, new features like voltage and frequency ride-through, to allow disturbance mitigation and dynamic grid support [37]. In the recent developments of SI, [38] proposed a detailed approach towards the realisation of autonomous, adaptive, cooperative, and plug-and-play functions in distributed environments. These characteristics allow SIs to act independently, make their choices, and do their jobs without being assisted. SIs facilitate stabilisation in the power systems and friendly communication features. As indicated in [39], the functions of stabilisation include: (1) connection/disconnection via grid, (2) power output control, (3) VAR control, (4) storage control, (5) event/history control, (6) status reporting/reading, and (7) time control. In the study [40], the desirable properties in SIs were categorised as autonomous or self-governing, self-adaptive, self-secure, and self-healing. The intelligent inverters must be intelligent enough to deal with faults, have self-healing features, adapt to changing conditions, and provide defense against possible cybersecurity attacks. All these make SIs very intelligent and efficient, and they work in harmony in the contemporary power systems. [41] touched upon the standards of communication of SI networks, such as high-level security, high scalability, low latency, and data rates.

Recent research has placed more emphasis on the imperative to advance inverter control and grid resilience strategies to compensate for the epochal penetration of DG of renewable energy. [42] proposed an adaptive method of the synchronverter control scheme where the virtual inertia and dampening factors are adjusted in real time in response to the system grid frequency error. In line with this, Bhowmik et al. studied the performance of LV grid resiliency under high renewable integration, comparing coordinated SI and demand-response algorithms. Their findings on renewable power generation revealed that reactive-power coordination and predictive-voltage management can reduce feeder-end voltage drops by more than 20% [43]. Regional-wise, [44] reviewed the strategies of SG implementation in Morocco, where communication limitations and regulatory differences have been found as the main obstacles in the implementation of a full SI. Their results emphasize the role of localized control structures and flexible standards of the power systems in North Africa. Taken together, these papers address a gap in the research between the design of the adaptive synchronverter and its implementation in the field in resource-constrained LV grids. The current research is a continuation of these findings with a more so-called refinement of a region that remains aligned to the proposed vision of an LS program, in addition to an energy-management system in Tunisia, to add regional relevance and further technical development to existing debates on how to manage grid stability.

2.1. Synchronverter: A Control Strategy of Grid-Forming Inverter

The synchronverter-based DG inverters, especially the PV systems, have been studied more on their capability to replicate SynGen to improve grid stability and renewable energy integration. They have been used specifically in PV systems and MGs and have proven to be reliable when operating in both grid-connected and islanded mode [45, 46]. Furthermore, synchronverter applications have extended to include High Voltage Direct Current (HVDC) transmission [47] and Static Synchronous Compensator (STATCOM) for voltage control and reactive power compensation [48, 49]. Currently, most of the grid-connected inverters operate in a grid-following mode, lacking the capability to function in islanding scenarios and support the grid during disturbances. Therefore, the emergence of grid-forming inverters is expected to improve power system dynamics by mitigating faults and enhancing stability while providing more autonomous and resilient operations. This makes them suitable for environments with less stable grids or those that incorporate more renewable energy sources. Therefore, the synchronverter technology is one of the grid-forming inverter techniques that emulate the virtual inertia of a SynGen [50, 51].

The synchronverter topology was well explained in the literature by Q.C. Zhong [52]. It is among the simplest and most performant virtual inertia emulation techniques, capable of operating in grid-connected and island modes. In this way, a synchronverter helps modern power systems address challenges in grid stability, frequency control, and dynamic response [53]. The synchronverter includes power and electronic parts. The power part consists of a three-phase, two-level DC/AC inverter with LCL filters, and the interface between the two parts is maintained through the voltage and current generated by the inverter.

The electronic part, illustrated in Figure 1, includes the controller, primarily operated through Pulse Width Modulation (PWM), and the signal generator that generates the reference signals the inverter should follow.

The basic equations below define the SynGen dynamic [52]:

$$T_e = M_f i_f \langle i, \widetilde{\sin\theta} \rangle \tag{1}$$

$$e = [e_a \;\; e_b \;\; e_c]^T = M_f i_f \dot{\theta}\, \widetilde{\sin\theta} \tag{2}$$

$$Q = -M_f i_f \dot{\theta} \langle i, \widetilde{\cos\theta} \rangle \tag{3}$$

$$\left.\begin{aligned} \widetilde{\sin\theta} &= \begin{bmatrix} \sin\theta \\ \sin\left(\theta - \frac{2\pi}{3}\right) \\ \sin\left(\theta - \frac{4\pi}{3}\right) \end{bmatrix} \;;\; i = \begin{bmatrix} i_a \\ i_b \\ i_c \end{bmatrix} \\ \widetilde{\cos\theta} &= \begin{bmatrix} \cos\theta \\ \cos\left(\theta - \frac{2\pi}{3}\right) \\ \cos\left(\theta - \frac{4\pi}{3}\right) \end{bmatrix} \end{aligned}\right\} \tag{4}$$

Where θ [rad] is the rotor angle, M_f [H] is the mutual inductance, i_f [A] is the field excitation current, and i [A] is the current vector consisting of the three-phase stator current i_a, i_b, and i_c. T_e [N. m] is the virtual electromagnetic torque, e [V] is the three-phase generated voltage vector comprising e_a, e_b, and e_c, and Q [VAR] is the reactive power of the synchronverter.

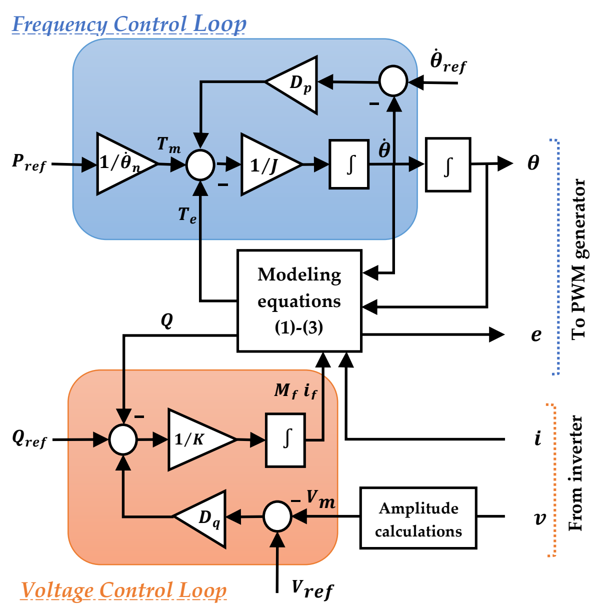

Fig. 1 The synchronverter control strategy

Figure 1 illustrates the two control loops of a synchronverter, ensuring frequency and voltage regulation in the event of a disturbance. The active power control loop, based on the swing Equation 5, regulates the angular frequency and the power angle of the reference voltage [52].

$$\frac{d\dot{\theta}}{dt} = \frac{1}{J}\left[T_m - T_e + D_p\left(\dot{\theta}_{ref} - \dot{\theta}\right)\right] \tag{5}$$

Where T_m [N. m] and T_e [N. m] are the mechanical and electromagnetic torques, respectively. J [kg · m^2] is the moment of inertia. $\dot{\theta}$ [rad/s] and $\dot{\theta}_{ref}$ [rad/s] are the synchronverter angular speed and reference angular speed, respectively.

To implement a synchronverter, the damping factor D_p [N. m. s/rad] and the moment of inertia J are calculated using Equations 6 and 7, where τ_f [s] refers to the time constant of active power control-based frequency regulation, ΔP [W] represents the variation in synchronverter power, and $\Delta\dot{\theta}$ [rad/s] denotes the change in the synchronverter angular speed.

$$D_p = -\frac{\Delta P}{\dot{\theta}\,\Delta\dot{\theta}} \tag{6}$$

$$\tau_f = \frac{J}{D_p} \tag{7}$$

The basic idea of the synchronverter is to mimic the SynGen inertia by using the energy stored in the DC-link capacitors of power converters connected to the grid.

Just like the case of H [s], which represents the SynGen inertia, the virtual inertia H_c [s] for DC-link capacitors C [F] with a rated voltage V_{dc} [V] is given by [54]:

$$H = \frac{J\dot{\theta}^2}{2S_{n\_Gen}} \tag{8}$$

$$H_c = \frac{CV_{dc}^2}{2S_{n\_Syn}} \tag{9}$$

Where S_{n_Gen} [VA] and S_{n_Syn} [VA] are the rated power of SynGen and synchronverter, respectively, the reactive power control loop regulates the excitation flux using the following equations [52]:

$$\frac{d}{dt}[M_f\, i_f] = \frac{1}{K}\left[Q_{ref} - Q + D_q(V_{ref} - V_m)\right] \tag{10}$$

$$\tau_v = \frac{K}{\dot{\theta}_n D_q} \tag{11}$$

Where Q [VAR] and Q_{ref} [VAR] are the reactive power and reference value of reactive power delivered by the inverter, respectively, D_q [kVAR/V] is the voltage droop coefficient, τ_v [s] is the time constant of the reactive power control-based voltage regulation, and K [kVAR. rad/V] is the gain for determining M_f i_f [A] (the product of mutual inductance and excitation current). V_{ref} [V] and V_m [V] are the reference voltage and the amplitude of the inverter voltage, respectively.

2.2. Volt-Var: A Control Strategy of Grid-Supporting Inverter

Previously, IEEE Std 1547 [55] banned reactive power support through DG. However, the most recent grid codes include requirements for reactive power control to support voltage regulation and grid stability. Thus, Volt-Var control has been integrated into such standards as IEEE Std 1547, recently published revision [36], and into various other regional initiatives like California's Rule 21 [35] and Hawaii's Rule 14H [56]. The main objective of the Volt-Var control is to keep voltage levels within a specified range to ensure a reliable operation of the electrical equipment and minimize voltage fluctuations. Accordingly, the Volt-Var function manages reactive power absorption when the voltage exceeds the upper threshold. Conversely, if the voltage decreases below the lower threshold, injecting reactive power into the distribution system assists in maintaining normal voltage levels.

The Volt-Var curve adopted by the IEEE Std 1547-2018 is displayed in Figure 2 [36]. In this case, the SI reactive power requirement Q [VAR] as a function of V [V] is expressed mathematically by Equation 12.

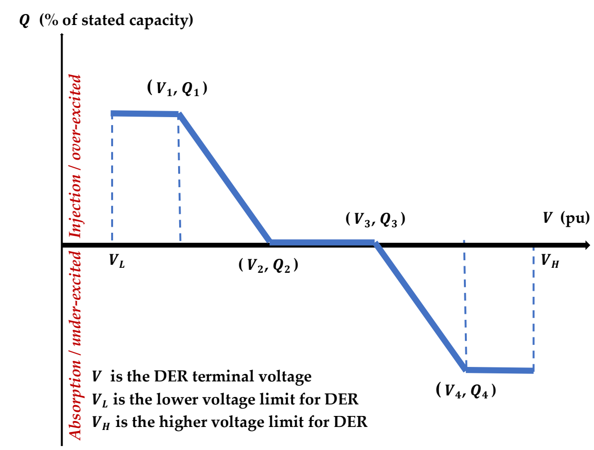

Fig. 2 Volt-Var characteristic [36]

$$Q(V) = \begin{cases} Q_1\,, & V \le V_1 \\ Q_2 + \dfrac{Q_1 - Q_2}{V_1 - V_2}(V - V_2)\,, & V_1 < V \le V_2 \\ 0\,, & V_2 < V \le V_3 \\ Q_3 + \dfrac{Q_4 - Q_3}{V_4 - V_3}(V - V_3)\,, & V_3 < V \le V_4 \\ Q_4\,, & V > V_4 \end{cases} \tag{12}$$

In this study, once the Volt-Var control is activated according to the proposed algorithm, it manages the synchronverter inputs to regulate the voltage levels effectively: the input of active power control-based frequency regulation is P_{ref} [W], and the input of reactive power control-based voltage regulation is Q_{ref} [VAR] (as shown in Figure 1).

Actually, priority is given to the reactive power exchange in the proposed strategy. To deliver the desired reactive power ($Q_{inv}^{max} = Q_1 = -Q_4$), it is necessary to reduce the active power output, particularly during periods of high active power generation, to prevent the inverter from becoming oversized. Consequently, if the condition is satisfied ($P_{inv}^{max} < S_{inv}$), the active power reference P_{ref} is set to the inverter's maximum active power P_{inv}^{max}, as defined by Equation 13. Otherwise, the active power reference is determined based on the power generated by the PV system (P_{PV} [W]).

$$P_{inv}^{max} = \sqrt{{S_{inv}}^2 - (Q_{inv}^{max})^2} \tag{13}$$

Where S_{inv} [VA], P_{inv}^{max} [W] and Q_{inv}^{max} [VAR] are the apparent power, the maximum active power, and the maximum reactive power of the inverter, respectively.

3. Load Shedding Use Case for the Tunisian LV Grid

The Smart Grid (SG) has been introduced as a new trend, resulting in a significant step towards a more sustainable and flexible energy system. Indeed, it provides a two-way flow for both energy and data owing to its energy, intelligence, and communication infrastructures. In this regard, the National Institute of Standards and Technology (NIST) has introduced the SG conceptual model, splitting it into seven interconnected domains: generation, transmission, distribution, operations, service providers, markets, and customers [57]. According to [58], the SG features a multi-layer architecture for implementation, consisting of 1) a power system layer, 2) a power control layer, 3) a communication layer, 4) a security layer, and 5) an application layer.

As part of the SG infrastructure, advanced power electronics and sensing technologies enhance energy management and demand control [59]. In addition to traditional functions of measuring and registering the amount of energy passing through the meter, Smart Meters (SMs) feature two-way communication, making it possible to transmit meter readings and remotely receive data. In this way, residents can save on electricity costs and reduce their electricity consumption, with the ability to switch the power supply on and off remotely [59, 61]. Communication infrastructure plays a crucial role in the SG. The collected data is modulated based on the communication protocol and transmitted wirelessly (by Bluetooth, ZigBee, Wi-Fi, WiMAX, etc.) or wired (by power line communication, optical fiber, Ethernet, etc.) to the management system. To transfer data, each SG domain has different communication links with several other domains, and each domain has its own network infrastructure. The Home Area Network (HAN) enables communication between devices, SMs, local generators, and electric vehicles at the customer's site. The SMs are connected to a Neighborhood Area Network (NAN) and then to a Wide Area Network (WAN) that links distribution, transmission, and bulk generation data [59, 61-63]. Touted as an important Advanced Metering Infrastructure (AMI) link, the data concentrator, in turn, connects the NAN and the WAN. The data concentrator gathers data from different meters collected via NAN and sends it to central utility servers through WAN [64]. Moreover, SMs can effectively establish Virtual Power Plants (VPPs) and ensure better commercial and technical management of DERs. First of all, a VPP can be defined as a group of multiple DERs. It allows the system operator to control different distributed elements through communication and coordination between the system operator and the DERs through a proper protocol. The smart energy management based on the DER management technology is identified as a strategic need for effective DER integration in the VPP, which is beneficial to both the distribution and transmission system operators. In this way, the system is made more flexible due to the collaboration of the various DERs [65-67].

As the object of the study, the Tunisian MG, which is an element of SG, with a communication infrastructure that has SMs, was chosen, as shown in Figure 3. Here, the MG will be able to work in grid mode and off-grid mode. It depends on hardware, e.g., SIs and switches, to regulate energy flow. Instead, the VPP is linked to the grid at all times through sophisticated software interlacing with the system operators. VPPs depend first of all on software, leveraging SMs and information technology to operate DER networks and take advantage of data analytics [68].

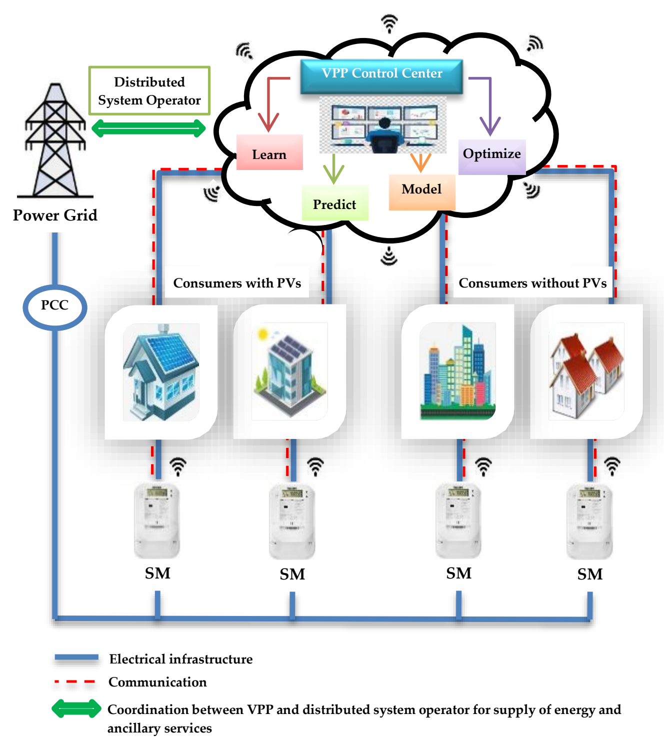

Fig. 3 General scheme of the proposed study

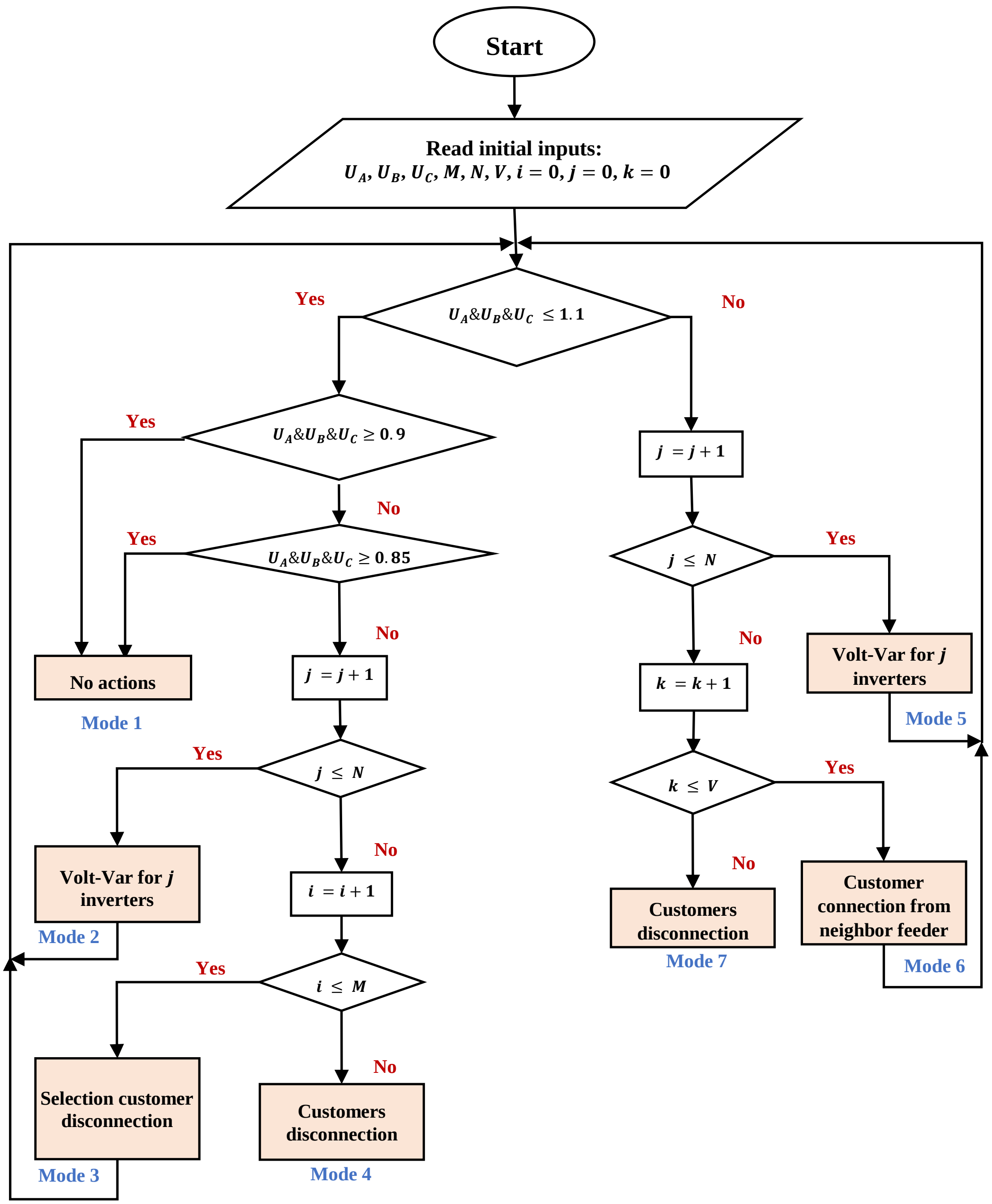

U_A, U_B, and U_C: Selected customer's three-phase reference voltage (p.u).
M: Number of single-phase customers on the feeder; **i**: Index of single-phase customers on the feeder.
V: Number of customers connected to the neighboring feeder; **k**: Index of customers connected to the neighboring feeder.
N: Number of PV systems; **j**: Index of the PV system's inverter.
No actions = Customers stay connected.
Customers disconnection = Customers whose voltage is not within acceptable limits, despite the algorithm's actions, will be disconnected remotely via SMs.

Fig. 4 Flowchart of the proposed MG-EMS

During the work with the inverters, the anti-islanding feature is frequently under the stringent standards and regulations, e.g., IEEE Std 1547-2003 [55], under which the safe working conditions are guaranteed, i.e., the solar systems do not provide electricity during the grid failures. Anytime such anomalies are detected by an inverter, the inverter terminates its connection with the grid. In this framework, islanding detection methods are effectively used for unintentional and intentional islanding to mitigate grid stability risks [69]. However, the 2018 updated version of IEEE 1547 allows intentional islanding, provided the system can accommodate it [36]. The study is particularly interested in the operational scenario relating to scheduled LS.

When switching to grid-disconnected mode, the connection to the grid on the transformer side is lost. Breakers are added between feeders initially open (in disconnected mode), and the algorithm gradually manages these breakers, closing them as needed. During the LS, the system shifts from grid-connected to grid-disconnected mode, also known as MG mode. In this case, instead of controlling the inverter in grid-connected mode, the synchronverter is activated. Even more, with a remote configuration of the inverter-connected PVs, the anti-islanding protection is disabled, and the permissible new voltage limits are set to 0.85 p.u. and 1.1 p.u., pending updates to the Tunisian grid code with a focus on the islanding study.

The proposed MG-EMS operates in seven modes, as shown in Figure 4. Mode 1 applies when voltage levels are maintained within the permissible limits, between 0.85 p.u. and 1.1 p.u., allowing the customers to remain connected without further actions. Modes 2, 3, and 4 are triggered when voltage levels drop below 0.85 p.u. In Mode 2, a Volt-Var control is implemented within the synchronverter to regulate the voltage. This control is activated sequentially, inverter-by-inverter, indexed by j. If necessary, up to N PV systems are activated based on the results of voltage level tests performed at each step. If Mode 2 proves insufficient, Mode 3 is enabled. Mode 4 is used to disconnect the customers whose voltage is beyond the acceptable limits, even with the actions of the algorithm, which uses SMs. Modes 5, 6, and 7 are concerned with the situation when the voltage levels exceed 1.1 p.u., i.e., Mode 5 is similar to Mode 2, and it switches the Volt-Var control inverter-by-inverter.

In Mode 6, instead of disconnecting customers, as in Mode 3, customers from neighboring feeders are connected to balance the load. The same principle from Mode 3 is applied, with a prioritization of low-consumption customers, starting with those closest to the transformer. This is because they have a more stable voltage, and reconnecting them first helps stabilize the network gradually. Finally, Mode 7 mirrors Mode 4, focusing on disconnecting loads whose voltage levels exceed the authorized limits.

4. Simulation Results and Discussion

4.1. Test Network Case Study

The tested network is a part of the Tunisian rural LV distribution network, configured as a radial network with different feeders. The single-line diagram of the studied network is displayed in Figure 5. The distribution feeders are linked to a 400 kVA transformer with a nominal voltage rating of $\frac{30}{0.42}$ kV. The supply line consists mainly of overhead lines carrying $\frac{420}{\sqrt{3}}$ V for each phase.

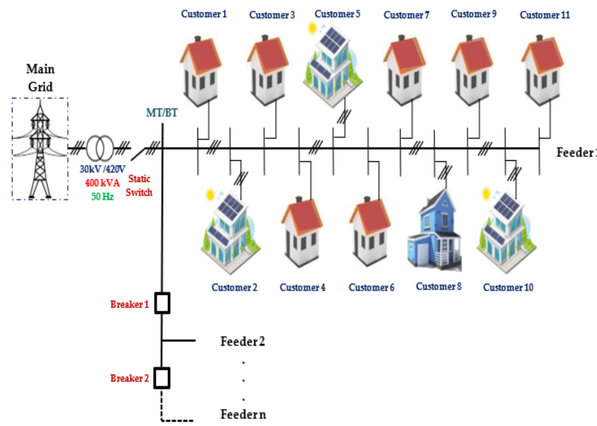

Fig. 5 Single-line diagram of the studied network

The MG connects to the power grid at the Point of Common Coupling (PCC) via a static switch, which opens during LS. Likewise, during LS, the added breakers between feeders are initially open, and the algorithm gradually closes these breakers as necessary. The research focused on modeling feeder 1 because, throughout the simulation of the studied scenario, the algorithm maintained the voltage value below 1.1 $p.u$, thus, eliminating the need to supply customers from neighboring feeders and keeping the breakers open. Feeder 1, as illustrated in the diagram, has 11 nodes supplying customers categorized as single-phase or three-phase, residential or non-residential, with or without PVs. A summary of the main parameters for each customer is provided in Table 1. Simulations were run to test the management strategy suggested, and they were performed in MATLAB/Simulink. Table 2 provides a summary of the main parameters and configurations of the SI, the synchronverter control, and the LV network. The sensitivity analysis was conducted as a parametric analysis, designed to assess the strength of the synchronverter control system. Each of the damping factor (D_p) and inertia constant (J) was perturbed over the nominal values (in 10 percent steps in each direction) to test system response under varying conditions. The voltages and frequency deviations at the PCC were observed. The outcomes demonstrated the resilience of the developed MG-EMS approach, as the suggested control strategy ensures stable voltage profiles and system stability even in the presence of parameter perturbations.

Table 1. Customer parameters

	D (m)	Customer Phase	S_c (kVA)	P_{pv} (kWp)
Customer 1	30	A	7	-
Customer 2	40	ABC	14	7
Customer 3	70	B	6.6	-
Customer 4	90	C	7	-
Customer 5	105	ABC	20	13
Customer 6	130	A	7	-
Customer 7	160	C	6	-
Customer 8	175	ABC	14	-
Customer 9	195	B	6	-
Customer 10	230	ABC	16	7
Customer 11	252	C	6.6	-

D is the distance from the transformer
Customer Phase refers to the phase at which the customer is connected.
S_c and P_{PV} are the customer-contracted power and the PV peak power, respectively.

The studied network is equipped with a communication infrastructure, enabling the aggregation of different DERs via SMs and the VPP, as shown in Figure 3. We, therefore, collected data on PV production and customer consumption on the summer day-ahead LS, modeling the 24-hour data over 10 seconds. Figures 6 and 7 display the load curves for single-phase and three-phase customers.

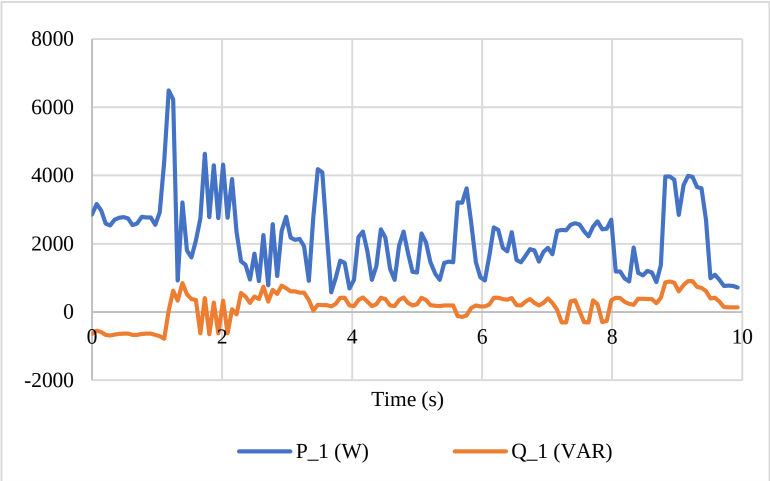

(a)

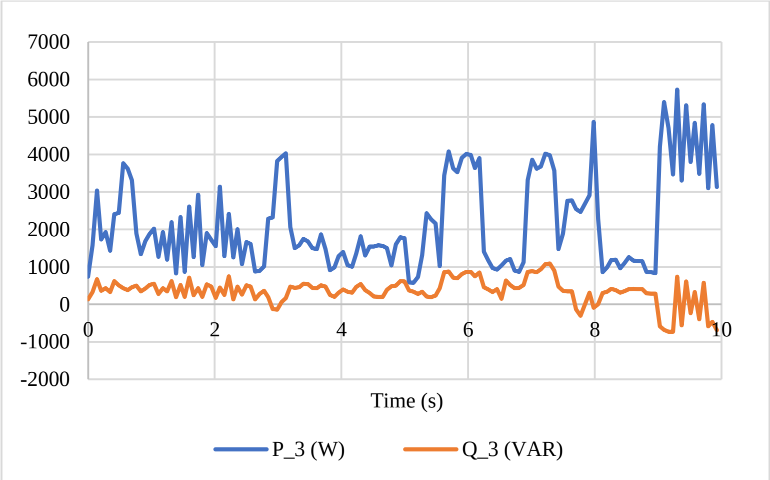

(b)

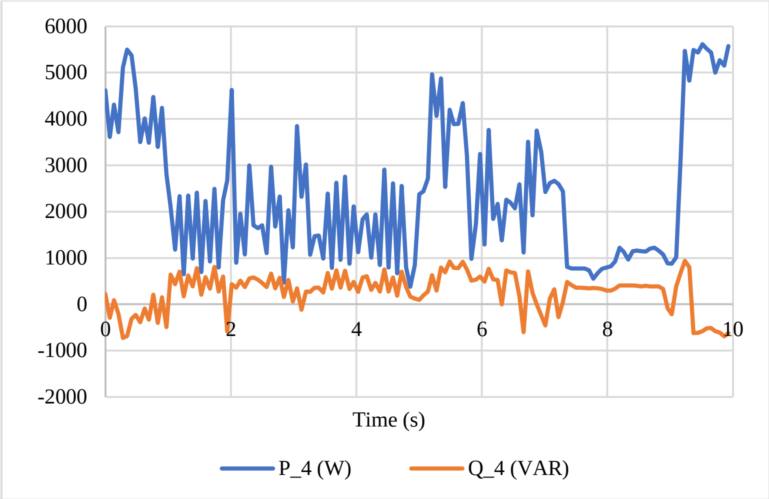
6000
5000
4000
3000
2000
1000
0
-1000
-2000
0
2
4
6
8
10
Time (s)
P_4 (W)
Q_4 (VAR)

(c)

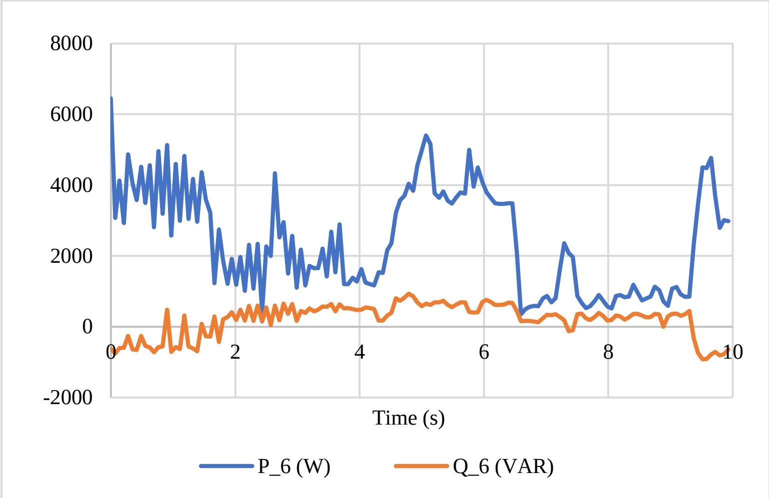
8000
6000
4000
2000
0
-2000
0
2
4
6
8
10
Time (s)
P_6 (W)
Q_6 (VAR)

(d)

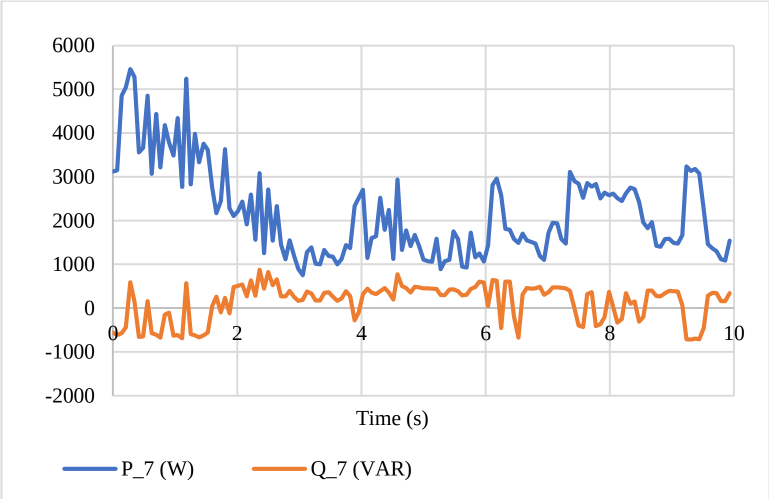
6000
5000
4000
3000
2000
1000
0
-1000
-2000
0
2
4
6
8
10
Time (s)
P_7 (W)
Q_7 (VAR)

(e)

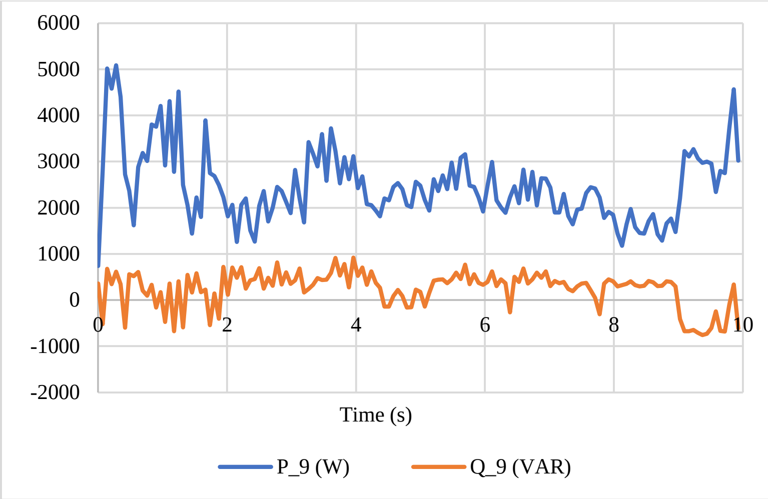

(f)

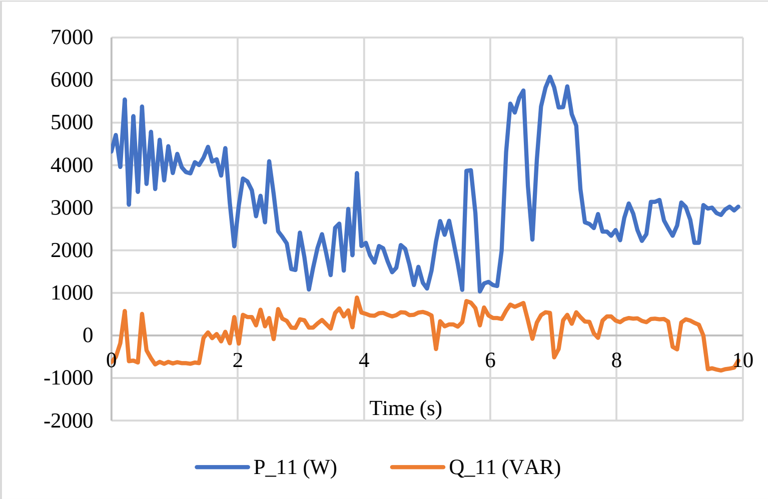

(g)

Fig. 6 Load curves for single-phase customers: (a) Customer 1, (b) Customer 3, (c) Customer 4, (d) Customer 6, (e) Customer 7, (f) Customer 9, and (g) Customer 11.

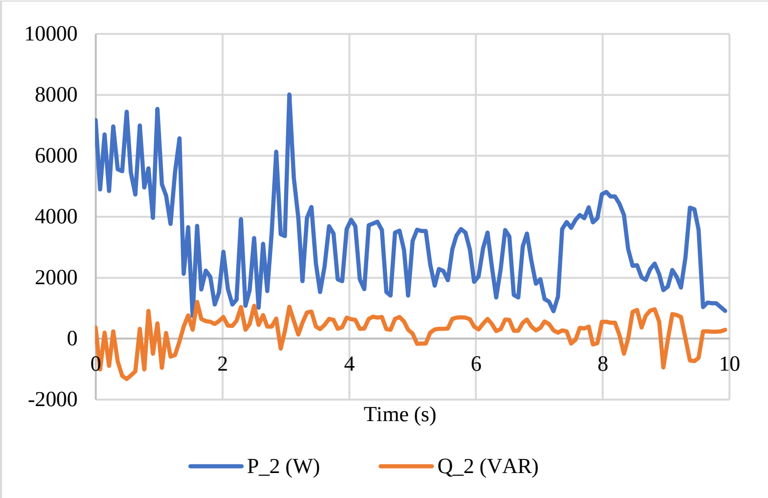

(a)

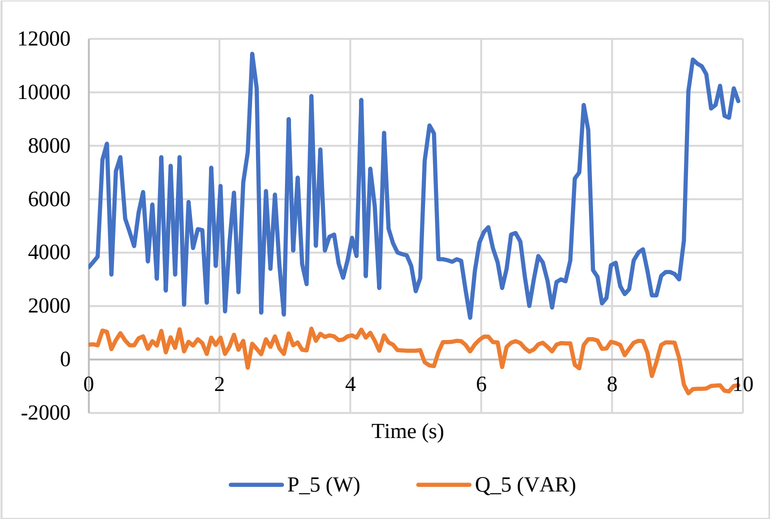

(b)

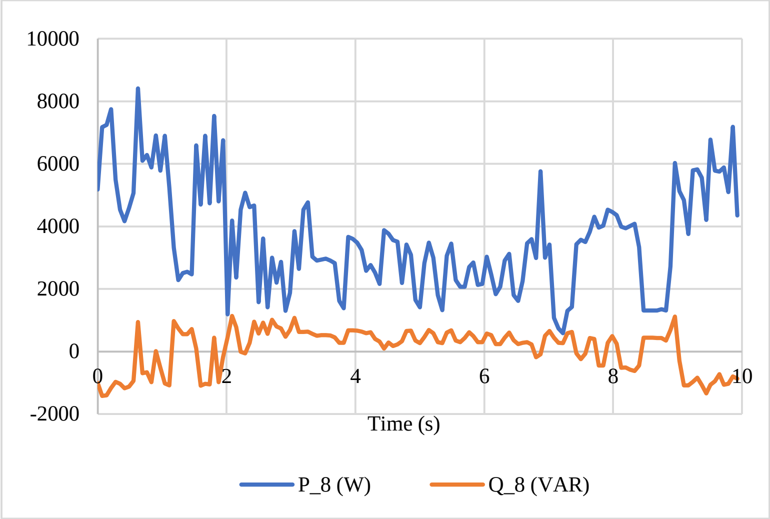

(c)

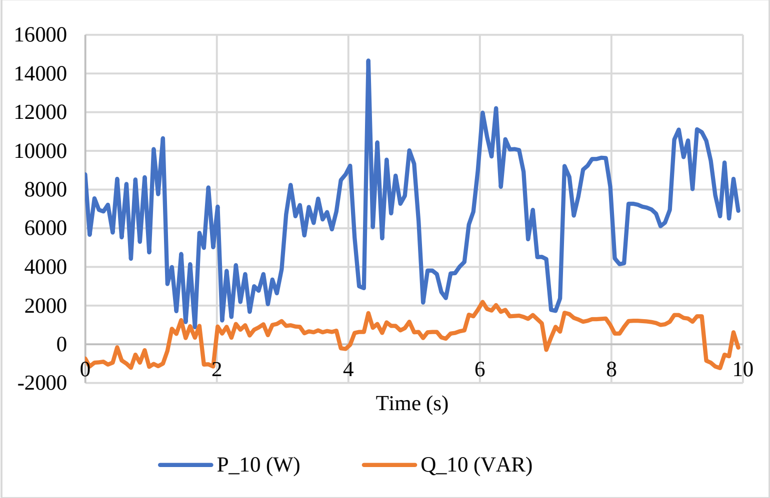

(d)

Fig. 7 Load curves for three-phase customers: (a) Customer 2, (b) Customer 5, (c) Customer 8, and (d) Customer 10.

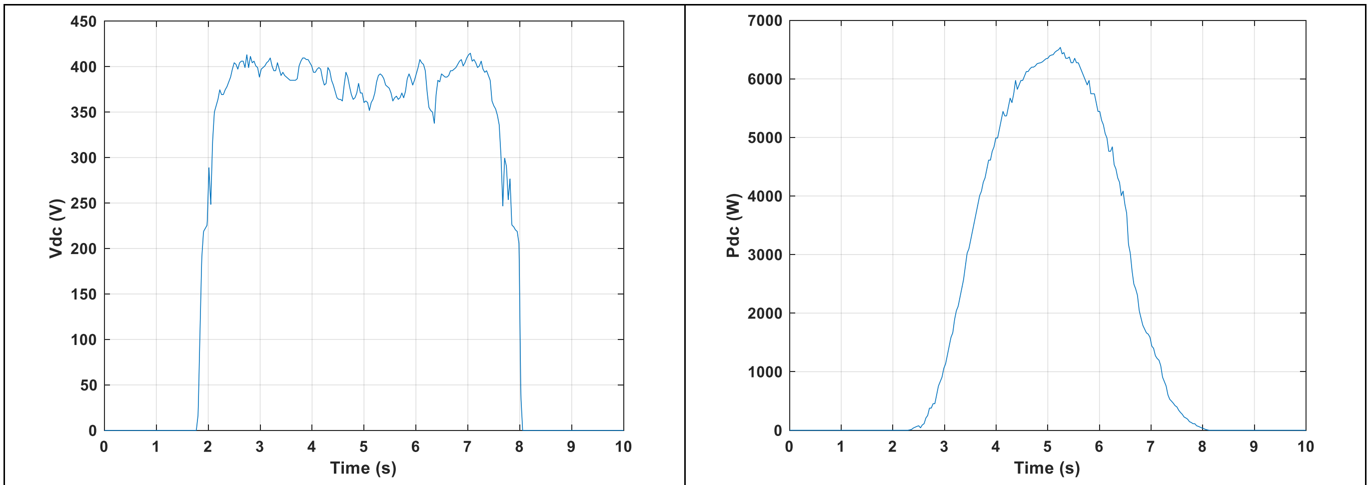

(a) (b)

Fig. 8 The PV installed at Customer 2: (a) Voltage, and (b) Generated power.

Figure 8 shows the power and voltage curves measured at the inverter input on the DC side for the 7 kWp PV of customer 2, selected to take its PCC voltage value as a reference for the MG-EMS based on an algorithm.

4.2. Results and Discussion

The simulation was carried out on the MATLAB/SIMULINK platform, with all results tested and validated against real electrical data to ensure an accurate and realistic analysis. The parameters of the controllers used in the SI are provided, along with a comprehensive description of the proposed algorithm for a programmed LS.

In fact, according to the Tunisian electricity grid code, the voltage limits for BT networks are set at a minimum of 0.9 p.u. and a maximum of 1.1 p.u. Referring to the Volt-Var characteristic in Figure 2, the V1 and V4 setpoints were set to the lower and upper statutory voltage limits for Tunisian LV distribution networks at 0.9 and 1.1 p.u. The V2 and V3 setpoints were adjusted to enable the inverter to inject reactive power until the voltage reached 0.98 p.u. and to absorb reactive power as the voltage approached 1 p.u. [36]. The synchronverter's parameters of Customer 2 are given in Table 2. Tunisia's peak consumption occurs between 10.30 a.m. and 4 p.m. The LS was scheduled for the next day. Two LS events were studied, each lasting 30 minutes. The first occurs at 10.48 a.m., corresponding to 4.5 seconds on the scale, where the 24-hour data was modeled over 10 seconds. The second event occurs at 2.24 p.m., corresponding to 6 seconds on the same scale.

Table 2. Simulation parameters in the proposed MG-EMS framework

Parameter	Symbol	Value / Description
Rated PV capacity	P_{PV}	7 kWp (Customer 2)
Nominal inverter apparent power	S_{inv}	8.5 kVA
Grid nominal voltage	V_{grid}	420 V (three-phase)
DC-link voltage	V_{dc}	620 V
Nominal grid frequency	f_{grid}	50 Hz
Filter inductance	L_s	10.831 mH
	L_g	1.338 mH
Series Resistors	R_s	1.66 Ω
	R_g	0.166 Ω
Filter capacitance	C	2.556 µF
	R_c in series with C	2.159 Ω
Damping factor	D_p	75 N. m. s/rad
Virtual inertia	J	0.15 kg. m^2
Voltage Droop Coefficient	D_q	100 kVAR/V
Frequency Loop Time Constant	τ_f	0.002 s
Voltage Loop Time Constant	τ_v	0.432 s
Switching frequency	F_s	10 kHz
Number of smart inverters	N	4 (three-phase customers)
Simulation duration	–	10 s (scaled 24-hour equivalent)

The proposed MG-EMS algorithm was applied during the two planned LSs. It was tested using an LS algorithm based on voltage regulation, as described above.

The MG-EMS algorithm aims to ensure the supply of certain priority loads during islanding, especially when LS is scheduled. Based on the experimental tests, Customer 2 is selected to take its PCC voltage value as a reference for the MG-EMS based on an algorithm. Careful consideration of the operational aims, including voltage stability, power quality, and generally system efficiency, promotes this choice.

Therefore, this sub-section examines the operation of an SI-based 7 kWp PV system at Customer 2 that is coupled to the Tunisian rural LV grid, as shown in Figure 5.

4.2.1. Case Study I: PV System Response without SI Integrating MG-EMS

The simulation started at $t = 0\ s$. Between 0 and 4.5 s, the inverter is in its normal operation, whereby current is injected into the grid by matching the grid voltage in the PLL. To attain synchronization, an AC bus reference voltage is necessary such that the inverter follows the grid in terms of voltage, frequency, and phase. In this way, the supplied power is compatible and does not harm the grid in any way. The inverter-linked PV is mainly programmed to inject the produced PV energy into the grid with the power factor being unity.

During the interval [0, 4.5 s], the main voltage and frequency remain within the permissible thresholds, specifically [47.5, 52 Hz] for frequency and [0.9, 1 p.u.] for voltage. The frequency remains within permissible limits during the [4.5, 4.708 s] period, albeit with fluctuating values. However, this is not the case for the voltages, as shown in Figures 9 (a) and 9 (d), which show the three-phase voltage curves at the inverter output in volts and at the customer's PCC in p.u., respectively. The research observes a voltage drop at the voltage level due to 'customer disconnect', caused by the shutdown of power generation from both the grid (which has been disconnected) and the PV system (due to anti-islanding protection). Consequently, as outlined in Figure 9 (b), the current at the inverter output drops to zero.

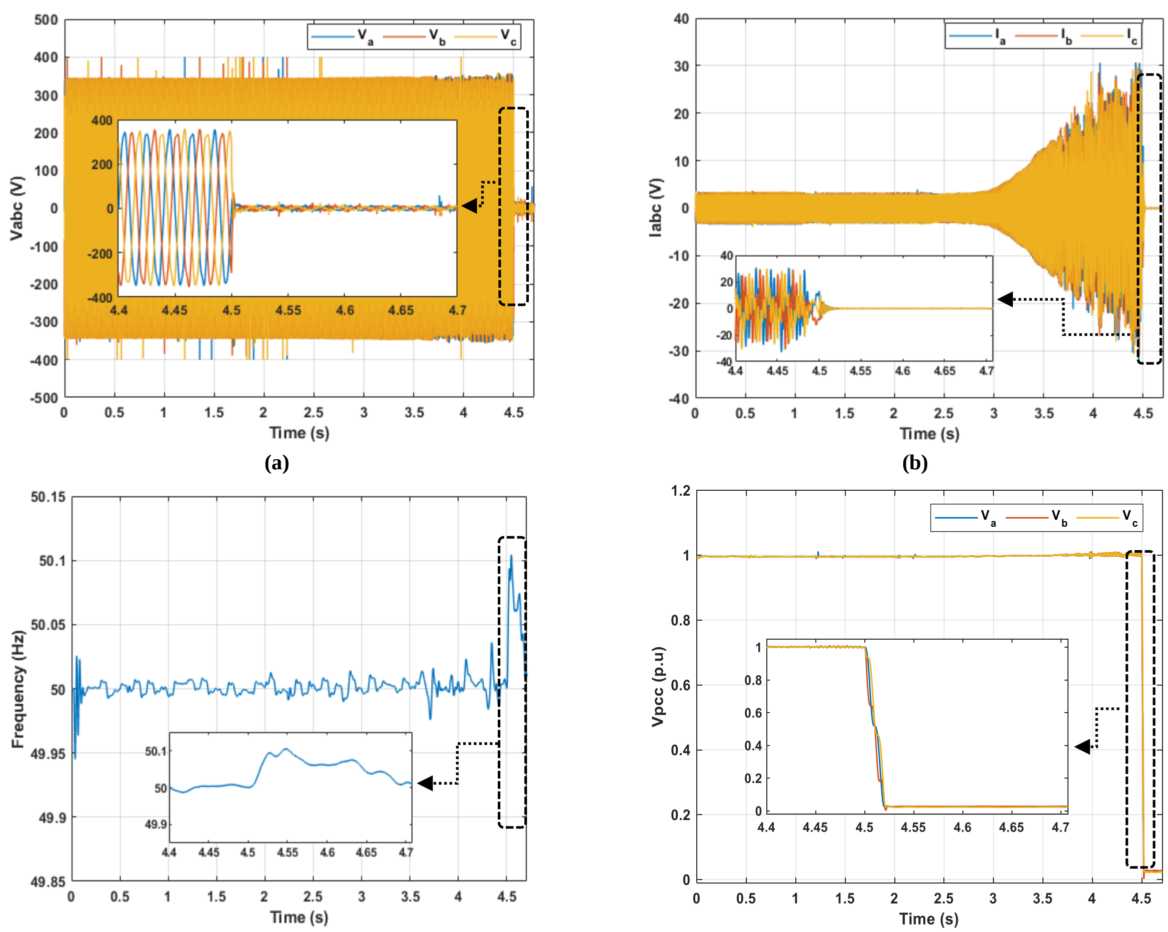

Fig. 9 Simulation results with grid-feeding inverter: (a) Inverter output voltage, (b) Inverter output current, (c) Inverter frequency, and (d) PCC voltage for Customer 2.

4.2.2. Case Study II: PV System Response with SI Integrating MG-EMS

Just as in case study I, the inverter followed the grid from 0 s to 4.5 s. At 4.5 s, a 30-minute scheduled LS was applied. Then, a second 30-minute LS was also applied at 6 s. To overcome the limitations of conventional inverter control, the study introduced SI, followed by the proposed management system known as MG-EMS.

This system incorporates an LS algorithm handling voltage regulation. The study explains the process during the two LS events. The proposed algorithm was applied the day ahead of the scheduled LS, using data gathered from SMs and VPPs regarding PV generation and customer consumption. The reference curves for active and reactive power at the synchronverter inputs were generated by activating Volt-Var, as detailed in Figures 10 and 11.

Based on customer consumption levels, priority indices were assigned to customers to identify the order of their disconnection. According to the priority order criterion for selecting customers to be disconnected, they were classified in the following order: Customer 11, Customer 9, Customer 7, Customer 6, Customer 4, Customer 3, Customer 1, Customer 8, Customer 10, Customer 5, and Customer 2. In Mode 3, the study disconnected the first two single-phase customers (Customer 11 and Customer 9) during the 4.5s LS event. For the second LS event at 6 s, the study expanded the disconnection to include the first four single-phase customers (Customer 11, Customer 9, Customer 7, and Customer 6) to maximize the number of customers served while ensuring that priority three-phase customers remained connected. On the scheduled day of LS, real-time monitoring of voltage levels for the remaining connected customers will be conducted. The SM can automatically disconnect the customer when permitted voltage thresholds are exceeded. Accordingly, only Mode 2 and Mode 3 were activated during the simulation.

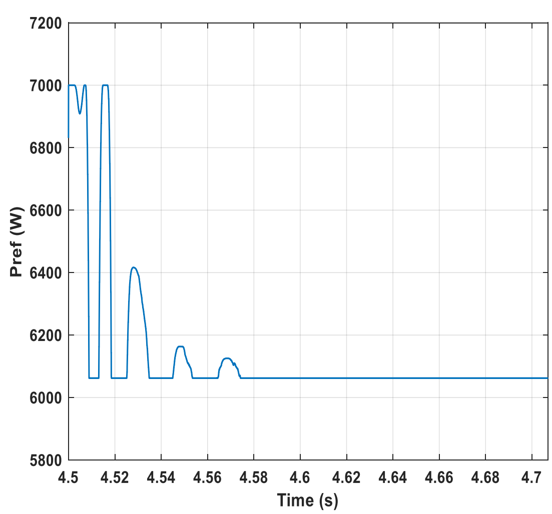

(a)

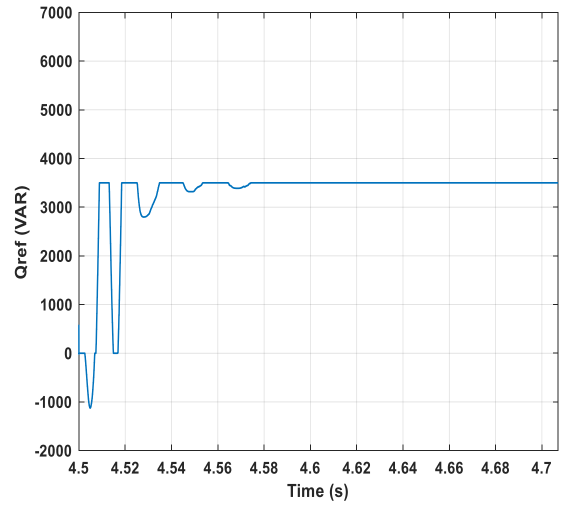

(b)

Fig. 10 Synchronverter inputs at 4.5 s : (a) Reference value of active power, and (b) Reference value of reactive power.

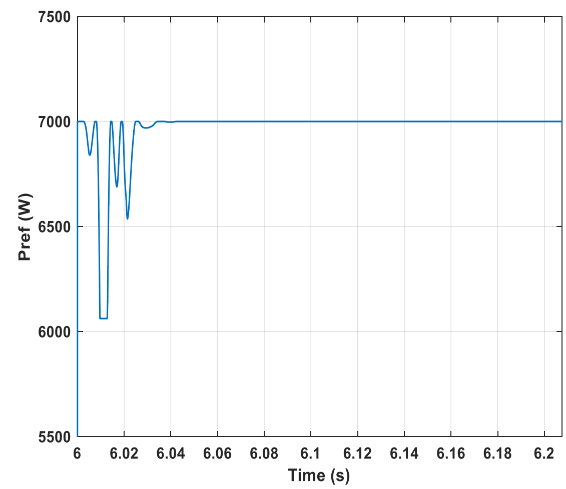

(a)

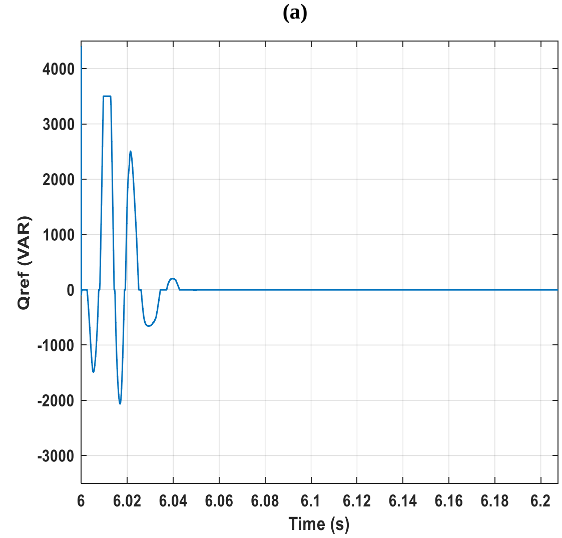

(b)

Fig. 11 Synchronverter inputs at 6 s : (a) Reference value of active power, and (b) Reference value of reactive power.

The inverter responses with SI and MG-EMS, based on a 7 kWp PV system installed at Customer 2, are presented in the curves of Figures 12 and 13. The frequency remains within permissible limits during the two LS periods [4.5, 4.708 s] and [6, 6.208 s]. During these reference times, the current is no longer zero but flows through the inverter as PV power is produced. Likewise, the voltage is maintained within permissible limits, avoiding the dips observed in case study I. This is illustrated in Figures 12 (b) and 13 (b), which show the three-phase voltage at the inverter output in volts, and Figures 12 (d) and 13 (d), which display the three-phase voltage at the customer's PCC in p.u. Figures 14 (a) and 15 (a) depict the three-phase generated voltage, also known as back electromotive force, marked by its sinusoidal form. Figures 14 (b) and 15 (b) outline the excitation current, representing the voltage control loop output of the synchronverter. The droop mechanism of the synchronverter was enabled during this process. In other words, the real power and reactive power delivered by the synchronverter did not follow the reference values, as shown in Figures 14 (c), 14 (d), 15 (c), and 15 (d). Instead, the synchronverter increased the real and reactive power outputs, trying to regulate the slight drops in voltage and frequency. Figures 16 and 17 show the PCC voltage profile for customers connected to feeder 1 during islanding periods. All voltage levels are within the new authorized limits, set at 0.85 p.u. and 1.1 p.u., pending updates of the Tunisian grid code dealing with islanding studies. Thus, the simulation results confirm the effectiveness of the proposed MG-EMS based on voltage regulation under weather changes and load variations.

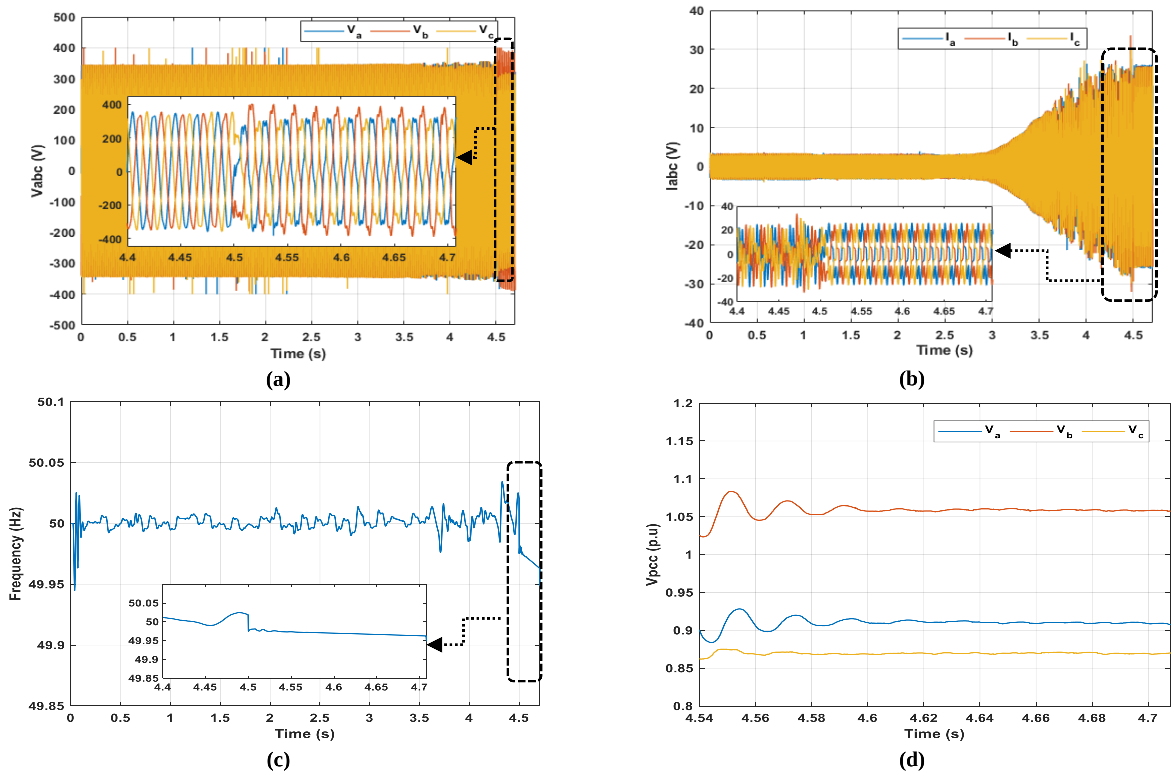

Fig. 12 Simulation results with MG-EMS from 4.5 s to 4.708 s : (a) Inverter output voltage, (b) Inverter output current, (c) Inverter frequency, and (d) PCC voltage for customer 2.

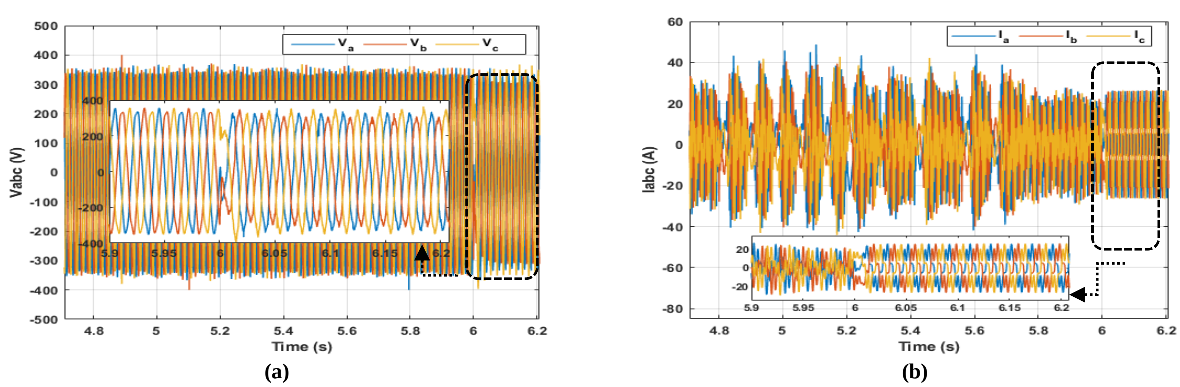

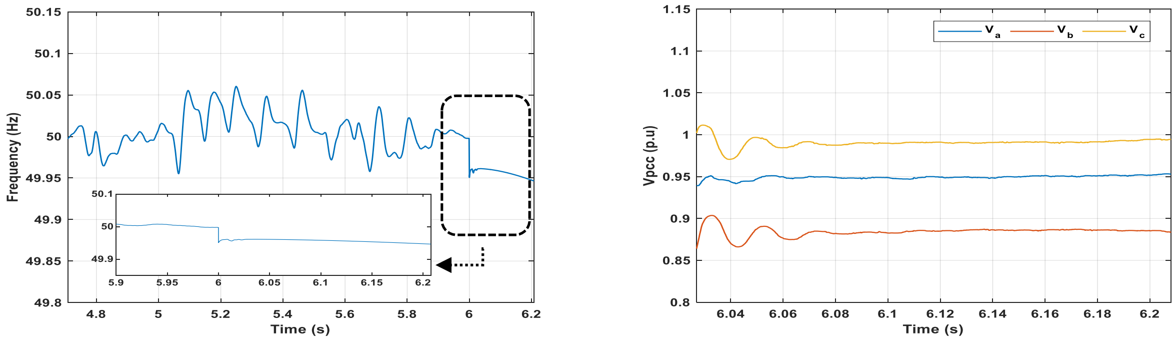

(c) (d)

Fig. 13 Simulation results with MG-EMS from 6 s to 6.208 s : (a) Inverter output voltage, (b) Inverter output current, (c) Inverter frequency, and (d) PCC voltage for customer 2.

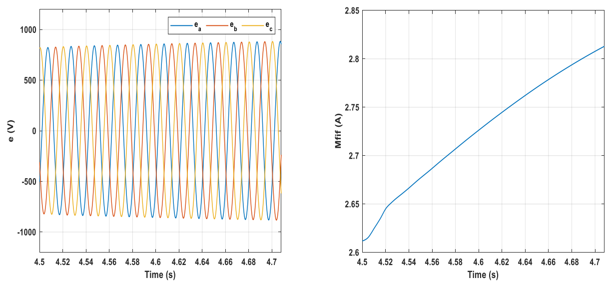

(a) (b)

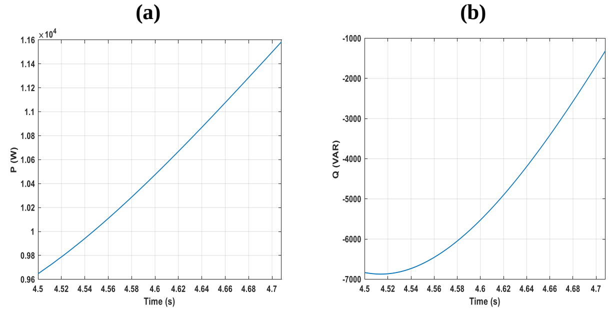

(c) (d)

Fig. 14 Synchronverter response at 4.5 s : (a) Three-phase generated voltage, (b) Excitation current, (c) Real power, and (d) Reactive power.

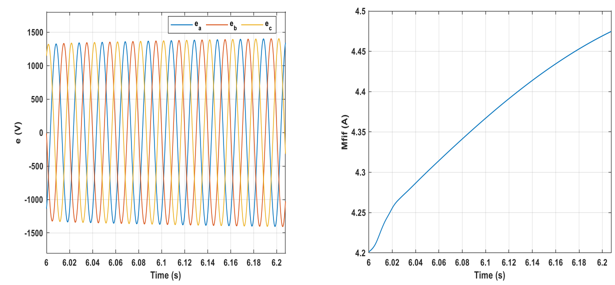

(a) (b)

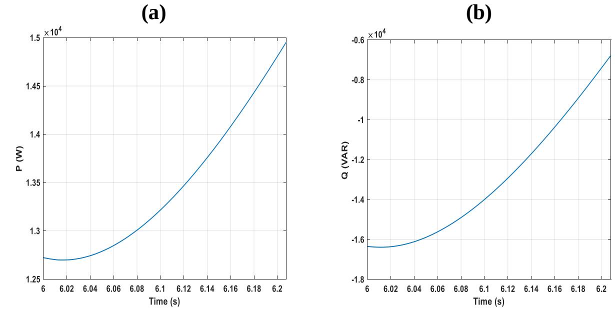

(c) (d)

Fig. 15 Synchronverter response at 6 s : (a) Three-phase generated voltage, (b) Excitation current, (c) Real power, and (d) Reactive power.

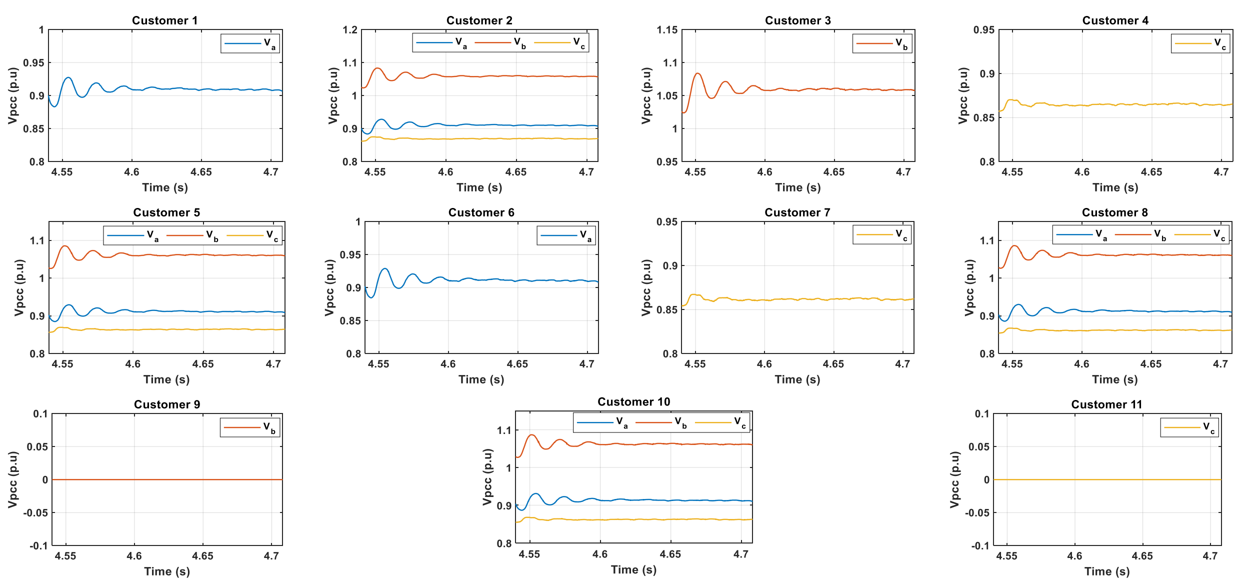

Fig. 16 PCC voltage for customers connected to Feeder 1 at 4.5 s

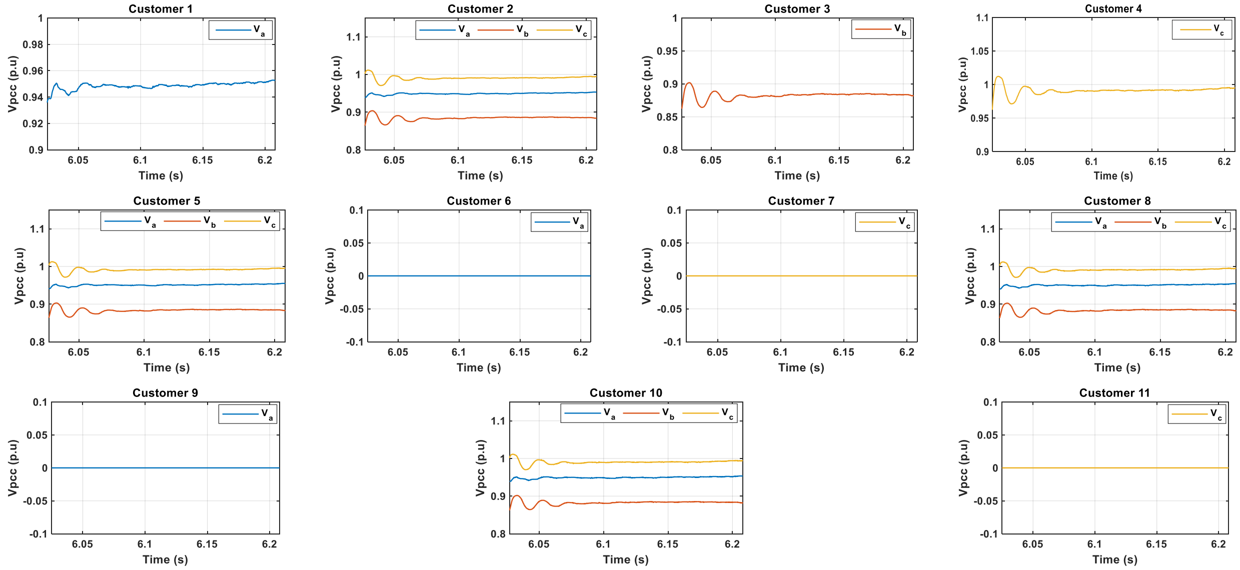

Fig. 17 PCC voltage for customers connected to Feeder 1 at 6 s

Based on the simulation results, using the SI integrating MG-EMS for Tunisia's LV distribution network, the main contributions of this study can be summarized as follows:

- Overcoming the limitation of conventional grid-feeding inverters.
- Dealing with Tunisia's energy deficit during LS periods via:

➢ The contribution of the available PV energy increases from 0% to 100%.

➢ The Customer Supply Rate (CSR), displayed in Figure 18 and expressed in Equation 14, shows the percentage of the successfully supplied customers.

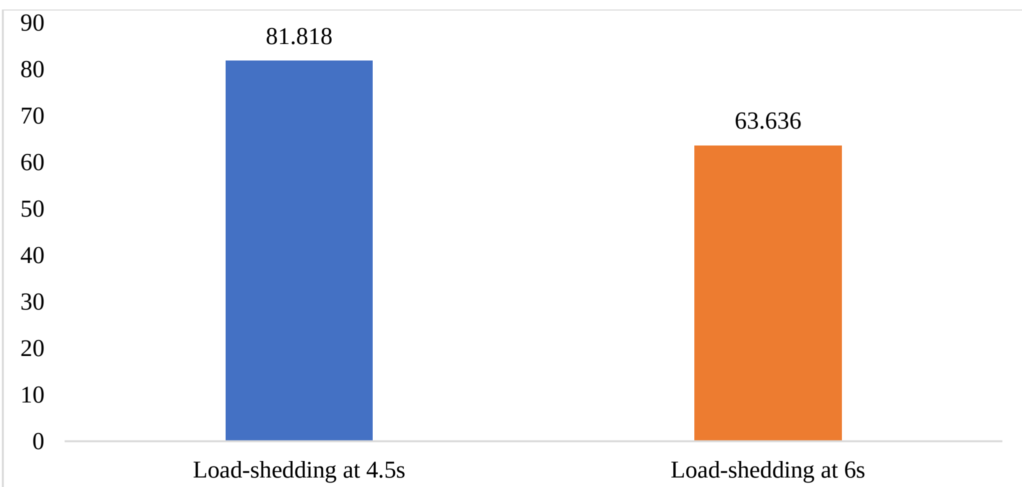

Fig. 18 The Customer Supply Rate with MG-EMS

$$CSR = \frac{N_C}{N_T} * 100 \quad (14)$$

Where N_C and N_T are the number of customers who remain connected and the total number of customers, respectively. Without integrating SI and MG-EMS, the CSR is 0%. However, the high CSR obtained from the simulation tests indicates that the algorithm effectively minimized disconnections, keeping as many customers as possible connected during LS.

5. Conclusion

Particularly, the suggested algorithm takes advantage of day-ahead data in order to plan LS in a way that retains customer voltage levels within the acceptable range, even during peak consumption times. Real-time monitoring during LS ensures the efficiency of the algorithm decisions. SMs check the voltage levels of customers who are still connected. In case the levels of voltage exceed the acceptable limits, the customer is disconnected remotely. The inverter control adjustments, including adjusting the allowable thresholds and the anti-islanding feature, can be disabled during scheduled LS, and this enables a smooth transition to islanded operation and improves the performance of the PV system. By applying strategies like Volt-Var and synchronverter controls, the system makes sure that the maximum number of customers stay connected, focusing on critical loads.

The possible focus of the future work will be on the dynamic LS analysis, which covers how fast the system responds to the grid disturbances and load changes.

In other words, it investigates unplanned LS situations. Through the use of artificial intelligence, the study will be able to predict load needs and PV generation precisely and proactively manage the energy needs through a more efficient approach. A cost-benefit analysis on the economic benefits of deploying SI and the long-term cost of energy savings is also required. Further research will be aimed at the experimental confirmation of the research under the conditions of dynamic load-shedding and proactive prediction of PV generation with the participation of AI to balance the grid.

Acknowledgments

The authors would like to express their gratitude to all people who took the time to share their knowledge in this study. Academic colleagues and reviewers are of special help. They made quite useful comments that enhanced the theoretical framework as well as the method applied in this work. The supervisors are also valued by the authors as the source of data that was used to support this research. It is also necessary to mention that no data was provided in the government service centres.

Nomeclature

AMI	Advanced Metering Infrastructure.	**PCC**	Point of Common Coupling.
ANME	National Agency for Energy Management.	**PLL**	Phase-Locked Loop.
CSR	Customer Supply Rate.	**PST**	Tunisian Solar Plan.
DER	Distributed Energy Resource.	**PV**	Photovoltaic.
DG	Distributed Generation.	**PWM**	Pulse Width Modulation.
EMS	Energy Management System.	**SG**	Smart Grid.
HAN	Home Area Network.	**SI**	Smart Inverter.
LS	Load-Shedding.	**SM**	Smart Meter.
LV	Low-Voltage.	**STEG**	Tunisian Company of Electricity and Gas.
MG	Microgrid.	**SynGen**	Synchronous Generator.
MG-EMS	Microgrid-Energy Management System.	**VPP**	Virtual Power Plant.
MV	Medium-Voltage.	**WAN**	Wide Area Network.
NAN	Neighborhood Area Network.		

References

[1] Noam Lior, "Sustainable Energy Development: The Present (2009) Situation and Possible Paths to the Future," *Energy*, vol. 35, no. 10, pp. 3976-3994, 2010. [CrossRef] [Google Scholar] [Publisher Link]

[2] Noam Lior, "Energy Resources and Use: The Present Situation and Possible Paths to the Future☆," *Energy*, vol. 33, no. 6, pp. 842-857, 2008. [CrossRef] [Google Scholar] [Publisher Link]

[3] E.C. Quaye, "Energy Demand in the 21st Century: The Role of Biofuels in a Developing Country," *Renewable Energy*, vol. 9, no. 1-4, pp. 1029-1032, 1996. [CrossRef] [Google Scholar] [Publisher Link]

[4] Omar Ellabban, Haitham Abu-Rub, and Frede Blaabjerg, "Renewable Energy Resources: Current Status, Future Prospects and their Enabling Technology," *Renewable and Sustainable Energy Reviews*, vol. 39, pp. 748-764, 2014. [CrossRef] [Google Scholar] [Publisher Link]

[5] IEA, Share of Cumulative Power Capacity by Technology, 2010-2027, Paris, France, 2022. [Online]. Available: https://www.iea.org/data-and-statistics/charts/share-of-cumulative-power-capacity-by-technology-2010-2027

[6] Snapshot of Global PV Markets 2023, International Energy Agency Photovoltaic Power Systems Programme, 2023. [Online]. Available: https://iea-pvps.org/wp-content/uploads/2023/04/IEA_PVPS_Snapshot_2023.pdf

[7] New Version of the Tunisian Solaire Plan, ANME, 2015. [Online]. Available: https://www.energiemines.gov.tn/fileadmin/user_upload/energies_renouvelables/PST_2015.pdf

[8] Action Plan for the Acceleration of Renewable Energy Projects in Tunisia, ANME, 2018. [Online]. Available: https://www.anme.tn/sites/default/files/2024-09/plan_daction_pour_lacceleration_des_projets_er_2018.pdf

[9] Tunisia, The Deutsche Gesellschaft für Internationale Zusammenarbeit (GIZ) GmbH has been Working in Tunisia Since 1970. It has had an office in the Capital, Tunis, since 1999, GIZ, 2026. [Online]. Available : https://www.giz.de/en/regions/africa/tunisia

[10] Tunisia's Energy Dependence Rate Stood at 48% at the End of June 2023, Business News, 2023. [Online]. Available: https://businessnews.com.tn/2023/08/15/article-1199745/1199745/

[11] Tunisian Ministry of Industry, Mines and Energy, Energy Situation, 2023. [Online]. Available: https://www.energiemines.gov.tn/fileadmin/docs-u1/Conjoncture_%C3%A9nerg%C3%A9tique_d%C3%A9cembre_2023___v_2024_.pdf

[12] Record Peak in Electricity Consumption in Tunisia: STEG Opts for Load Shedding, Managers, 2023. [Online]. Available: https://managers.tn/2023/07/21/pic-record-de-consommation-delectricite-en-tunisie-la-steg-opte-pour-le-delestage-electrique/

[13] No Automatic Load Shedding: STEG Confirms its Preparations for Summer 2024, The Press, 2024. [Online]. Available: https://www.turess.com/fr/lapresse/1191086

[14] Felix Rehmann et al., "District Energy Management Systems: Key Data Points for System Integration and Related Challenges: Lessons Learned from Experts in Germany," *Energy Technology*, vol. 12, no. 7, pp. 1-15, 2024. [CrossRef] [Google Scholar] [Publisher Link]

[15] C.F. Calvillo et al., "Impact of EV Penetration in the Interconnected Urban Environment of a Smart City," *Energy*, vol. 141, pp. 2218-2233, 2017. [CrossRef] [Google Scholar] [Publisher Link]

[16] J.A. Peças Lopes et al., "Integrating Distributed Generation into Electric Power Systems: A Review of Drivers, Challenges and Opportunities," *Electric Power Systems Research*, vol. 77, no. 9, pp. 1189-1203, 2007. [CrossRef] [Google Scholar] [Publisher Link]

[17] Sara Eftekharnejad et al., "Impact of Increased Penetration of Photovoltaic Generation on Power Systems," *IEEE Transactions on Power Systems*, vol. 28, no. 2, pp. 893-901, 2012. [CrossRef] [Google Scholar] [Publisher Link]

[18] Tariq Aziz, and Nipon Ketjoy, "PV Penetration Limits in Low Voltage Networks and Voltage Variations," *IEEE Access*, vol. 5, pp. 16784-16792, 2017. [CrossRef] [Google Scholar] [Publisher Link]

[19] Bruno de Nadai Nascimento et al., "Load Shedding Scheme with Under-Frequency and Undervoltage Corrective Actions to Supply High Priority Loads in Islanded Microgrids," *IET Renewable Power Generation*, vol. 13, no. 11, pp. 1981-1989, 2019. [CrossRef] [Google Scholar] [Publisher Link]

[20] Nur Najihah Abu Bakar et al., "Microgrid and Load Shedding Scheme during Islanded Mode: A Review," *Renewable and Sustainable Energy Reviews*, vol. 71, pp. 161-169, 2017. [CrossRef] [Google Scholar] [Publisher Link]

[21] Raja Masood Larik, Mohd Wazir Mustafa, and Muhammad Naveed Aman, "A Critical Review of the State-of-Art Schemes for under Voltage Load Shedding," *International Transactions on Electrical Energy Systems*, vol. 29, no. 12, pp. 1-26, 2019. [CrossRef] [Google Scholar] [Publisher Link]

[22] Hassan Haes Alhelou et al., "An Overview of UFLS in Conventional, Modern, and Future Smart Power Systems: Challenges and Opportunities," *Electric Power Systems Research*, vol. 179, 2020. [CrossRef] [Google Scholar] [Publisher Link]

[23] L.O. Mogaka, G.N. Nyakoe, and M.J. Saulo, "Power Prioritization and Load Shedding in an Island with RESs using ABC Algorithm," *Journal of Engineering*, vol. 2020, no. 1, pp. 1-10, 2020. [CrossRef] [Google Scholar] [Publisher Link]

[24] Sharman Sundarajoo, and Dur Muhammad Soomro, "Under Voltage Load Shedding and Penetration of Renewable Energy Sources in Distribution Systems: A Review," *International Journal of Modelling and Simulation*, vol. 43, no. 6, pp. 1002-1020, 2023. [CrossRef] [Google Scholar] [Publisher Link]

[25] Irtaza M. Syed, and Kaamran Raahemifar, "Predictive Energy Management and Control System for PV System Connected to Power Electric Grid with Periodic Load Shedding," *Solar Energy*, vol. 136, pp. 278-287, 2016. [CrossRef] [Google Scholar] [Publisher Link]

[26] Ruben Zieba Falama et al., "A Solution to the Problem of Electrical Load Shedding using Hybrid PV/Battery/Grid-Connected system: The Case of Households' Energy Supply of the Northern Part of Cameroon," *Energies*, vol. 14, no. 10, pp. 1-23, 2021. [CrossRef] [Google Scholar] [Publisher Link]

[27] Muhammad Paend Bakht et al., "A Community Scale Hybrid Renewable Energy System for Sustainable Power Supply during Load Shedding," *Indonesian Journal of Electrical Engineering and Computer Science*, vol. 31, no. 1, pp. 33-43, 2023. [CrossRef] [Google Scholar] [Publisher Link]

[28] Joan Rocabert et al., "Control of Power Converters in AC Microgrids," *IEEE Transactions on Power Electronics*, vol. 27, no. 11, pp. 4734-4749, 2012. [CrossRef] [Google Scholar] [Publisher Link]

[29] Allal M. Bouzid et al., "A Survey on Control of Electric Power Distributed Generation Systems for Microgrid Applications," *Renewable and Sustainable Energy Reviews*, vol. 44, pp. 751-766, 2015. [CrossRef] [Google Scholar] [Publisher Link]

[30] Arangarajan Vinayagam et al., "PV Based Microgrid with Grid-Support Grid-Forming Inverter Control-(Simulation and Analysis)," *Smart Grid and Renewable Energy*, vol. 8, no. 1, pp. 1-30, 2016. [CrossRef] [Google Scholar] [Publisher Link]

[31] Wei Du et al., "Modeling of Grid-Forming and Grid-Following Inverters for Dynamic Simulation of Large-Scale Distribution Systems," *IEEE Transactions on Power Delivery*, vol. 36, no. 4, pp. 2035-2045, 2020. [CrossRef] [Google Scholar] [Publisher Link]

[32] Zheng Zeng et al., "Topologies and Control Strategies of Multi-Functional Grid-Connected Inverters for Power Quality Enhancement: A Comprehensive Review," *Renewable and Sustainable Energy Reviews*, vol. 24, pp. 223-270, 2013. [CrossRef] [Google Scholar] [Publisher Link]

[33] Yaosuo Xue et al., "Towards Next Generation Photovoltaic Inverters," *IEEE Energy Conversion Congress and Exposition*, Phoenix, AZ, USA, pp. 2467-2474, 2011. [CrossRef] [Google Scholar] [Publisher Link]

[34] Yaosuo Xue et al., "On a Future for Smart Inverters with Integrated System Functions," *9th IEEE International Symposium on Power Electronics for Distributed Generation Systems (PEDG)*, Charlotte, NC, USA, pp. 1-8, 2018. [CrossRef] [Google Scholar] [Publisher Link]

[35] Electric Rule 21: Generating Facility Interconnections, California Public Utilities Commission, 2025. [Online]. Available: https://www.cpuc.ca.gov/Rule21/

[36] "1547-2018 - IEEE Standard for Interconnection and Interoperability of Distributed Energy Resources with Associated Electric Power Systems Interfaces," *IEEE*, pp.1-138, 2018. [CrossRef] [Google Scholar] [Publisher Link]

[37] Umid M. Mamadaminov, "Advanced Inverters and their Functionalities for Distributed Solar Generation," *Energy Engineering III*, Spring 2014. [Google Scholar]

[38] Yaosuo Xue, and Josep M. Guerrero, "Smart Inverters for Utility and Industry Applications," *Proceedings of PCIM Europe 2015; International Exhibition and Conference for Power Electronics, Intelligent Motion, Renewable Energy and Energy Management*, Nuremberg, Germany, pp. 277-284, 2015. [Google Scholar] [Publisher Link]

[39] Kushan Tharuka Lulbadda, and K.T.M.U. Hemapala, "The Additional Functions of Smart Inverters," *AIMS Energy*, vol. 7, no. 6, pp. 971-988, 2019. [Google Scholar]

[40] Behrooz Mirafzal, and Aswad Adib, "On Grid-Interactive Smart Inverters: Features and Advancements," *IEEE Access*, vol. 8, pp. 160526-160536, 2020. [CrossRef] [Google Scholar] [Publisher Link]

[41] Babak Arbab-Zavar et al., "Smart Inverters for Microgrid Applications: A Review," *Energies*, vol. 12, no. 5, pp. 1-22, 2019. [CrossRef] [Google Scholar] [Publisher Link]

[42] Emmanuel Torres Montalvo, Victor M. Sanchez, and Juan M. Ramirez, "Synchronverter Assessment for the Frequency Regulation of Control Areas Encompassing Renewable Distributed Generation," *International Journal of Hydrogen Energy*, vol. 46, no. 51, pp. 26138-26151, 2021. [CrossRef] [Google Scholar] [Publisher Link]

[43] Biddut Bhowmik, Moses Amoasi Acquah, and Sung-Yul Kim, "Hybrid Compatible Grid Forming Inverters with Coordinated Regulation for Low Inertia and Mixed Generation Grids," *Scientific Reports*, vol. 15, pp. 1-27, 2025. [CrossRef] [Google Scholar] [Publisher Link]

[44] Meryem Meliani et al., "Smart Grid Implementation in Morocco: Case Study," *Materials Today Proceedings*, vol. 45, pp. 7675-7679, 2021. [CrossRef] [Google Scholar] [Publisher Link]

[45] Ajinkya J. Sonawane, and Amod C. Umarikar, "Three-Phase Single-Stage Photovoltaic System with Synchronverter Control: Power System Simulation Studies," *IEEE Access*, vol. 10, pp. 23408-23424, 2022. [CrossRef] [Google Scholar] [Publisher Link]

[46] K.S. Raja Shekhar, and M.A. Chaudhari, "Operation and Control of Synchronverter Technique in Grid Connected and Intentional Islanding Modes for AC Micro Grids," *2020 First International Conference on Power, Control and Computing Technologies (ICPC2T)*, Raipur, India, pp. 426-431, 2020. [CrossRef] [Google Scholar] [Publisher Link]

[47] Raouia Aouini et al., "Synchronverter-Based Emulation and Control of HVDC Transmission," *IEEE Transactions on Power Systems*, vol. 31, no. 1, pp. 278-286, 2016. [CrossRef] [Google Scholar] [Publisher Link]

[48] Emanuel Leonardus van Emmerik, "*Synchronverter Applied to Power Systems*," Ph.D. Thesis, Federal University of Rio de Janeiro, Brazil, 2018. [Google Scholar] [Publisher Link]

[49] Ajinkya J. Sonawane, and Amod C. Umarikar, "Voltage and Reactive Power Regulation with Synchronverter-Based Control of PV-STATCOM," *IEEE Access*, vol. 11, pp. 52129-52140, 2023. [CrossRef] [Google Scholar] [Publisher Link]

[50] Ujjwol Tamrakar et al., "Virtual Inertia: Current Trends and Future Directions," *Applied Sciences*, vol. 7, no. 7, pp. 1-29, 2017. [CrossRef] [Google Scholar] [Publisher Link]

[51] Dayan B. Rathnayake et al., "Grid Forming Inverter Modeling, Control, and Applications," *IEEE Access*, vol. 9, pp. 114781-114807, 2021. [CrossRef] [Google Scholar] [Publisher Link]

[52] Qing-Chang Zhong, and George Weiss, "Synchronverters: Inverters That Mimic Synchronous Generators," *IEEE Transactions on Industrial Electronics*, vol. 58, no. 4, pp. 1259-1267, 2010. [CrossRef] [Google Scholar] [Publisher Link]

[53] Krishnakumar R. Vasudevan et al., "Synchronverter: A Comprehensive Review of Modifications, Stability Assessment, Applications and Future Perspectives," *IEEE Access*, vol. 8, pp. 131565-131589, 2020. [CrossRef] [Google Scholar] [Publisher Link]

[54] Jingyang Fang et al., "On the Inertia of Future More-Electronics Power Systems," *IEEE Journal of Emerging and Selected Topics in Power Electronics*, vol. 7, no. 4, pp. 2130-2146, 2018. [CrossRef] [Google Scholar] [Publisher Link]

[55] 1547-2003 - IEEE Standard for Interconnecting Distributed Resources with Electric Power Systems, *IEEE*, pp.1-28, 2003. [CrossRef] [Google Scholar] [Publisher Link]

[56] Anderson F. Hoke, "*Smart Inverter Utility Experience in Hawaii*," National Renewable Energy Lab. (NREL), USA, 2019. [Google Scholar]

[57] Chris Greer et al., "NIST Framework and Roadmap for Smart Grid Interoperability Standards, Release 3.0," *NIST Special Publication 1108r3*, 2014. [CrossRef] [Google Scholar] [Publisher Link]

[58] Murat Kuzlu, Manisa Pipattanasomporn, and Saifur Rahman, "Communication Network Requirements for Major Smart Grid Applications in HAN, NAN and WAN," *Computer Networks*, vol. 67, pp. 74-88, 2014. [CrossRef] [Google Scholar] [Publisher Link]

[59] Yasin Kabalci, "A Survey on Smart Metering and Smart Grid Communication," *Renewable and Sustainable Energy Reviews*, vol. 57, pp. 302-318, 2016. [CrossRef] [Google Scholar] [Publisher Link]

[60] Xi Fang et al., "Smart Grid - The New and Improved Power Grid: A survey," *IEEE Communications Surveys & Tutorials*, vol. 14, no. 4, pp. 944-980, 2011. [CrossRef] [Google Scholar] [Publisher Link]

[61] K.S.K. Weranga, S. Kumarawadu, and D.P. Chandima, *Smart Metering Design and Applications*, 1st ed., Springer Singapore, 2014. [CrossRef] [Publisher Link]

[62] Folasade Dahunsi et al., "Communication Network Simulation for Smart Metering Applications: A Review," *Journal of Innovative Science and Engineering*, vol. 5, no. 2, pp. 101-128, 2021. [CrossRef] [Google Scholar] [Publisher Link]

[63] Kanar Al-Sammak, Sama AL-Gburi, and Ion Marghescu, "Communications Systems in Smart Metering: A Concise Systematic Literature Review," *2022 14th International Conference on Communications (COMM)*, Bucharest, Romania, pp. 1-9, 2022. [CrossRef] [Google Scholar] [Publisher Link]

[64] Punya Prakash, "Data concentrators: The Core of Energy and Data Management," *Texas Instruments*, 2013. [Google Scholar]

[65] Mahmoud M. Othman, Y.G. Hegazy, and Almoataz Y. Abdelaziz, "A Review of Virtual Power Plant Definitions, Components, Framework and Optimization," *International Electrical Engineering Journal*, vol. 6, no. 9, pp. 2010-2024, 2015. [Google Scholar]

[66] Juan C. Sarmiento-Vintimilla et al., "Applications, Operational Architectures and Development of Virtual Power Plants as a Strategy to Facilitate the Integration of Distributed Energy Resources," *Energies*, vol. 15, no. 3, pp. 1-28, 2022. [CrossRef] [Google Scholar] [Publisher Link]

[67] Sambeet Mishra et al., *Virtual Power Plants and Integrated Energy System: Current Status and Future Prospects*, Handbook of Smart Energy Systems, Springer, 2023, pp. 115-145. [CrossRef] [Google Scholar] [Publisher Link]

[68] Jiaqi Liu et al., "Virtual Power Plant with Renewable Energy Sources and Energy Storage Systems for Sustainable Power Grid-Formation, Control Techniques and Demand Response," *Energies*, vol. 16, no. 9, pp. 1-28, 2023. [CrossRef] [Google Scholar] [Publisher Link]

[69] Reza Bakhshi-Jafarabadi et al., "Review on Islanding Detection Methods for Grid-Connected Photovoltaic Systems, Existing Limitations and Future Insights," *IET Renewable Power Generation*, vol. 16, no. 15, pp. 3406-3421, 2022. [CrossRef] [Google Scholar] [Publisher Link]